Tectonophysics 760 (2019) 199–220

Contents lists available at ScienceDirect

Tectonophysics

journal homepage: www.elsevier.com/locate/tecto

A review of large low shear velocity provinces and ultra low velocity zones

Allen K. McNamara

Department of Earth and Environmental Sciences, Michigan State University, 288 Farm Lane, Rm 207, East Lansing, MI 48824, United States

ARTICLE INFO

Keywords:
Lower mantle
Mantle convection
Large low shear velocity provinces
Ultra low velocity zones
Thermochemical convection

ABSTRACT

Seismic tomography reveals 2 extensive regions in the lowermost mantle, beneath Africa and the Pacific, that exhibit lower-than-average seismic wave speeds. These regions have been named the Large Low Shear Velocity Provinces (LLSVPs), and they have spatial scales on the order of 1000s and 100s of kilometers in width and height, respectively. Discovering their cause remains an important challenge in the deep Earth community because recognizing what they are has important, first-order implications toward understanding the nature of global mantle convection and therefore, heat and chemical transport and evolution through time. At about an order-of-magnitude smaller scale are Ultra Low Velocity Zones (ULVZs) that reside on the core-mantle boundary. ULVZs are typically up to 100s of kilometers laterally and only 10s of kilometers vertically. We don't know what LLSVPs and ULVZs are, and the primary question is whether they are thermal or compositional features, and/or both. In any case, there is every reason to suppose that they are linked by a dynamical relationship, and by better understanding one, we can discover more about the other. Here, we review the observations associated with LLSVPs and the various conceptual mantle models that the community is debating regarding their cause. ULVZs, as they may relate to the larger LLSVPs, are also reviewed, and dynamical linkages between the two are discussed. Better understanding both LLSVPs and ULVZs promises to provide critical insight into global scale mantle convection and therefore provide a foundation for understanding numerous other processes in the Earth's interior.

1. Introduction

Since the discovery of plate tectonics about 50 years ago, we've learned a considerable amount about the kinematics of plate motions, from the formation of plates at divergent spreading centers to their ultimate subduction into the mantle at convergent boundaries. However, convection in the Earth's mantle, the driving force behind plate tectonics, remains somewhat more enigmatic. We are still striving to discover the fundamental nature of large-scale mantle convection. Is the mantle compositionally heterogeneous? If so, how does that heterogeneity affect convective motions and thermal transport? Does the mantle convect as a single, relatively homogeneous layer, or do multiple scales of convection occur within separate partial layers or reservoirs? Does compositional heterogeneity affect the locations and sizes of convection cells or how temporally stable they are? How do we reconcile the differences in trace element chemistry between basalts formed at hotspots versus those formed at mid ocean ridges? Does the mantle consist of separate chemical reservoirs, and if so, how do they interact with each other, and how do they interact with mantle plumes that can bring their chemistry to the surface? These are but a few of the major scientific questions we are currently trying to answer. Of equal importance is discovering how we can use observations of seismology, geochemistry, and petrology, along with understanding gained by mineral physics, to answer these scientific questions.

Fig. 1 provides cartoons that illustrate several conceptual models of mantle convection that the community is currently debating. At first glance, there are very noticeable commonalities between these models. They each involve some kind of large-scale heterogeneity in the lower mantle beneath Africa and the Pacific. These structures are motivated by tomographic observations and have been named “Large Low Shear Velocity Provinces” (or LLSVPs for short). Furthermore, the cartoons illustrate African and Pacific LLSVPs having smaller-scale mantle plumes rising from them, an idea motivated by the numerous hotspots located at the surface above them. Finally, the cartoons show LLSVPs bounded by subducting slabs, again motivated by tomography. The major differences between various conceptual models (not all of which are visible from the cartoons) illustrate where most of the current debate is focused and is mostly caused by lack of conclusive observations. Firstly, it is unclear how voluminous the LLSVPs are and how far upward they rise into the mantle. It is unclear how well they are delineated from the surrounding, background mantle (e.g., how sharp their boundaries are), particularly along their tops. It is unclear whether they each are contiguous objects or poorly-imaged collections of smaller anomalies. Conceptual models differ in terms of what LLSVPs are made

E-mail address: allenmc@msu.edu.

https://doi.org/10.1016/j.tecto.2018.04.015
Received 1 August 2017; Received in revised form 18 April 2018; Accepted 24 April 2018
Available online 30 April 2018
0040-1951/

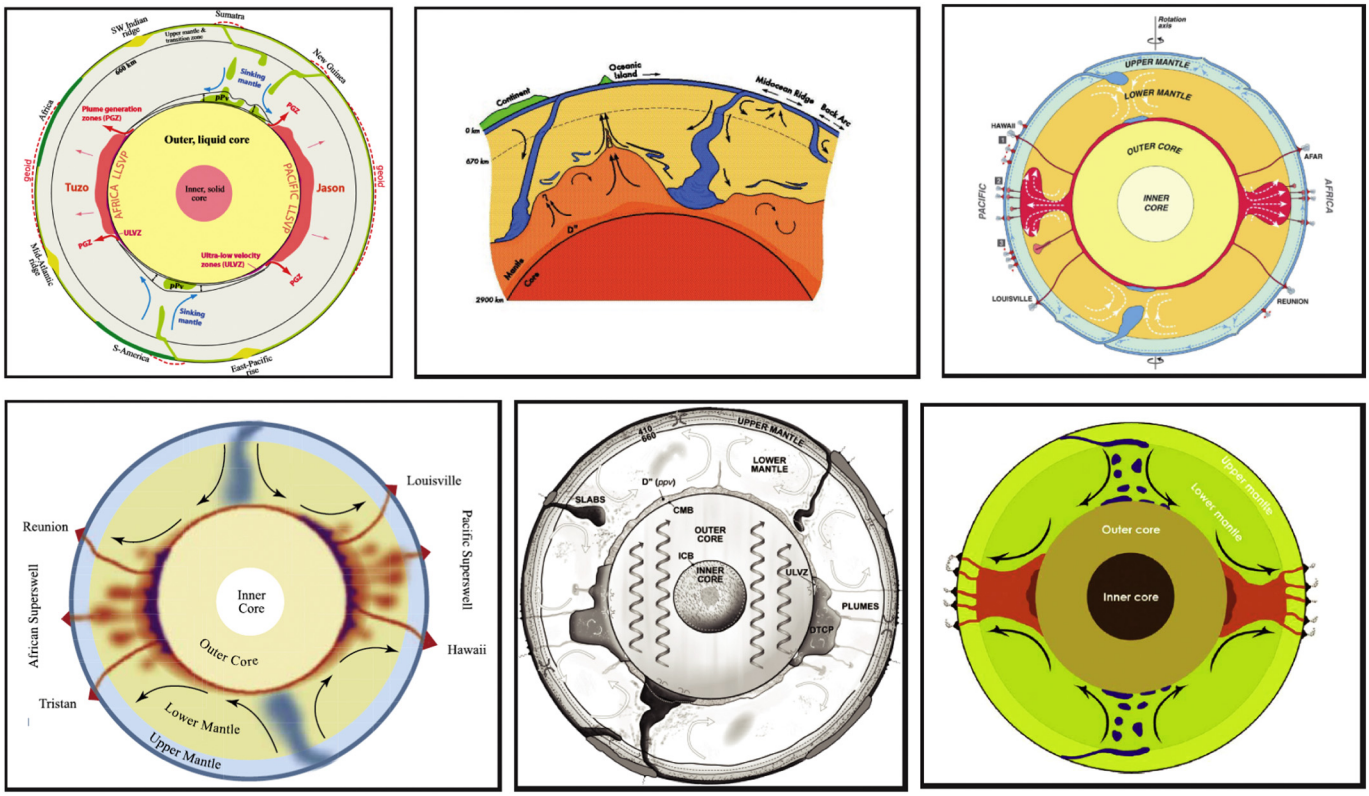

Fig. 1. Several conceptual models of mantle convection currently discussed in the solid-Earth community.
Figures are modified from the following sources, clockwise starting from the top left. **Top-left**: Torsvik et al. (2014). **Top-middle**: Kellogg et al. (1999). **Top-right**: Courtillot et al. (2003). **Bottom-left**: Jellinek and Manga (2004). **Bottom-middle**: Garnero et al. (2005). **Bottom-right**: Dziewonski et al. (2010).

of. Are they simply thermal anomalies or do they have a different composition from surrounding mantle? Conceptual models disagree with regard to LLSVP buoyancy and mobility. Are LLSVPs actively rising, or do they passively reside at the core-mantle boundary? Do they move around, laterally along the core-mantle boundary or are they relatively fixed in place? Conceptual models often also differ in terms of what caused LLSVPs in the first place and whether they have remained intact throughout geologic time, or whether they are in the process of being created or destroyed. Also related, the differences in the cartoons also illustrate our lack of understanding with regard to subducted slabs in the lower mantle, particularly whether slabs make it to the core-mantle boundary uninterrupted or whether they deflect and possibly break apart in the mid mantle.

The above differences between conceptual models lead to fundamentally different consequences toward our understanding of mantle convection, how it cools the Earth and stirs chemical heterogeneity, and ultimately drives plate tectonics. Heat transport and thermal evolution would differ greatly between these different ideas. Each conceptual model would exhibit a different style of chemical evolution, impacting our understanding of how the differences in hotspot and mid-ocean ridge basalt geochemistry are achieved. Any attempt to understand hotspots and how they could be caused by mantle plumes is directly and critically affected by knowing which of these different foundational frameworks are valid for Earth. Each conceptual model implies somewhat different driving forces of mantle convection and therefore impacts our understanding of how mantle convection drives plate tectonics. Finally, because the mantle is a boundary condition to the core, each of these models, with their differing insulating effects on the core, has different consequences toward understanding core heat loss and the geodynamo. In summary, discovering the first-order nature of global-scale mantle convection is prerequisite to and required for understanding a large host of important processes.

Discovering what the LLSVPs are and how they operate dynamically is a requirement toward understanding global mantle convection, which provides a first-order framework for subsequent understanding of the numerous structures and dynamics in the mantle and at the surface. Therefore, this review will first focus on the LLSVPs, starting with what we know about them through observations. It will then review the various end-member conceptual models (hypotheses) that the community has developed to explain them. Following that, the discussion will shift toward some of the smallest-scale structures we observe in the lowermost mantle, Ultra Low Velocity Zones (ULVZs for short). Although we don't understand what ULVZs are, we are confident to suppose that they must be related to the large-scale LLSVPs somehow, and therefore perhaps, some of the smallest-scale features in the mantle may provide strong insight into the nature of global-scale dynamics.

2. LLSVP observations

By definition, LLSVPs are an observation from shear-wave tomography. However, we've come to associate them with other observations as well, such as anomalies observed in compressional-wave (i.e., P-wave) tomography, regions of anti- or non-correlation between shear and bulk modulus observed in joint-inversion tomography studies, areas of anomalous density in normal mode studies, and regions surrounded by sharp wave speed gradients in travel-time and waveform studies. Furthermore, these regions are correlated with an increased number of hotspots on the surface above them and quite possibly the surface paleo-locations of hotspots in the past. This latter observation prompts a connection between LLSVPs, mantle plumes, hotspots, and geochemical reservoirs.

2.1. Seismic observations

The best tool we have to view the Earth's interior is seismic

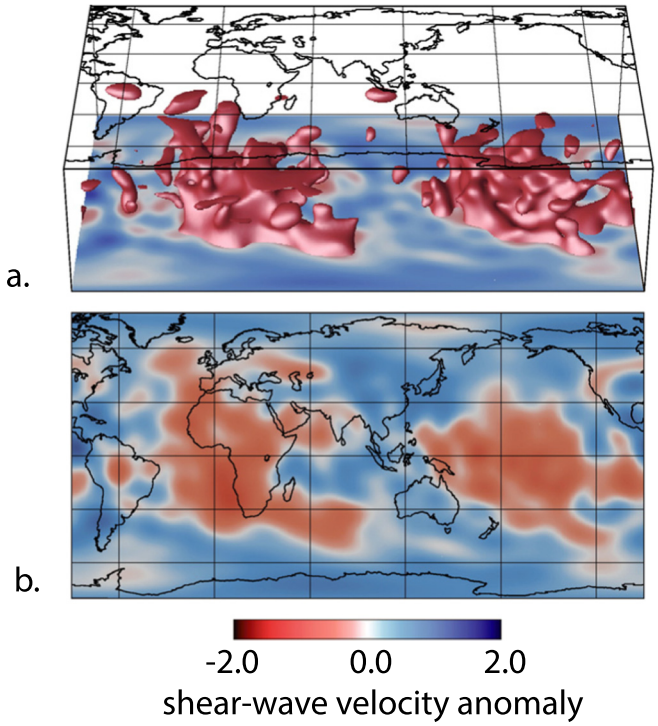

Fig. 2. Large Low Shear Velocity Provinces (LLSVPs).
Shear-wave tomography model S20RTS (Ritsema et al., 1999, 2004). **a.** Isosurface (red) representing −0.6% shear-wave anomaly throughout the mantle. The bottom of the Cartesian box is the core-mantle boundary. **b.** Map view in the lowermost mantle, at 2750 km depth. Figure modified from Bull et al. (2009). (For interpretation of the references to color in this figure legend, the reader is referred to the web version of this article.)

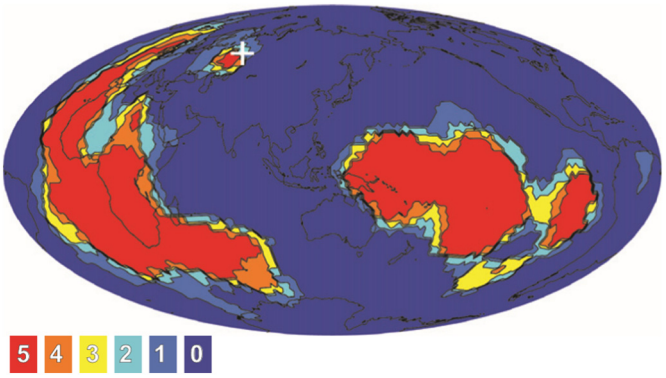

Fig. 3. Vote map, showing LLSVP consistency between shear-wave tomography models.
Taken from Lekic et al. (2012). The map is the result of a cluster analysis, comparing the lower-than-average anomalies in 5 models (Houser et al., 2008; Kustowski et al., 2008; Megnin and Romanowicz, 2000; Ritsema et al., 2011; Simmons et al., 2010). The depth range of comparison is 1000–2800 km depth. Color is defined by the number of models that agree in that particular region, as indicated by the numbered boxes.

tomography, and it has long provided first-order clues toward understanding interior structure and dynamics (e.g., Dziewonski et al., 1977). Fig. 2 illustrates a lowermost mantle map view and a lower mantle 3D image from shear-wave tomography model S20RTS (e.g., Ritsema et al., 1999, 2004). Higher-than-average shear wave speeds are observed beneath regions of paleosubduction (e.g., the circum-Pacific and Tethyian convergence beneath Eurasia). It is well-agreed that these are likely subducted slabs, remnants of slabs, and/or mantle cooled by slabs. Two, nearly antipodal regions of the lowermost mantle, beneath Africa and the Pacific, are characterized by lower-than-average shear wave speeds, and it is these anomalously slow regions that are referred to as the Large Low Shear Velocity Provinces (LLSVPs). LLSVPs are robust features, consistently observed in other shear-wave tomography models as well (e.g., French and Romanowicz, 2015; Grand, 2002; Houser et al., 2008; Kustowski et al., 2008; Li and Romanowicz, 1996; Megnin and Romanowicz, 2000; Ritsema et al., 2011; Ritsema et al., 1999, 2004; Simmons et al., 2010; Takeuchi, 2007). Lekic et al. (2012) performed a cluster analysis on five shear wave tomography models, effectively identifying the regions where models agree in terms of faster or slower than average wave speeds (Fig. 3). Furthermore, shear wave velocity maps from normal mode studies also show them (e.g., Ishii and Tromp, 1999, 2001, 2004; Mosca et al., 2012; Trampert et al., 2004). While details vary between models due to different techniques and datasets, they all basically agree in the existence of LLSVPs, their locations, and their general geometric shape in map view.

While shear-wave tomography models agree with each other reasonably well, there is more variability between compressional-wave tomography models (e.g., Becker and Boschi, 2002; Houser et al., 2008; Koelemeijer et al., 2016; Li et al., 2008; Simmons et al., 2010). This is not entirely surprising given the higher sensitivity of shear wave speed to temperature. Garnero et al. (2016) examined three different joint-inversion tomography models that simultaneous solved for both shear and compressional wave speeds. They found that the shear-wave parts of the models largely agree with each other in terms of LLSVP shape and position. Although the compressional-wave parts of the models vary widely from each other, it is visibly clear that their lowest velocities are mostly in the LLSVP regions. In other words, it can be argued that compressional-wave models also have large low velocity provinces, but when comparing them to LLSVPs, there is less agreement regarding their shape, length-scales, geographical locations, and anomaly amplitudes (Fig. 4).

The disagreements between LLSVPs and the low velocity anomalies in compressional-wave models may provide some important insight into how their composition differs from the surrounding mantle. The comparison is best done through joint-inversions that employ the same dataset and methods, in which a bulk sound velocity can be computed from a linear combination of shear and compressional wave speeds to isolate the bulk modulus. Once the bulk sound velocity is computed it can be correlated with the shear velocity to provide information on how homogenous the mantle is. In a homogenous material, the shear wave speed and the bulk sound wave speed are expected to vary together in the same manner as a function of temperature (at a given pressure). Therefore, if the lowermost mantle is homogeneous, we expect maps of shear-wave speed and bulk sound speed to look similar (although at different amplitudes). However, in the lowermost 500 km of the lower mantle, there appears to be a non- or perhaps even negative correlation between them (e.g., Antolik et al., 2003; Koelemeijer et al., 2016; Masters et al., 2000; Ritsema and van Heijst, 2002; Su and Dziewonski, 1997; van der Hilst and Karason, 1999). This is best explained by the presence of compositional heterogeneity or a phase change (e.g., post-perovskite) (e.g., Koelemeijer et al., 2016), as the difference between elastic moduli will be different for each composition. Furthermore, the lowest wave speeds in shear-wave models tend to cover a larger geographic area than those in compressional-wave models in the lowermost 700 km of the mantle, inferring the presence of compositional heterogeneity (Hernlund and Houser, 2008). The presence of lowermost mantle compositional heterogeneity is also supported by statistical and probabilistic tomography studies that use thermodynamic relationships from mineral physics to extract temperature and composition from shear- and compressional-wave inversions (e.g., Deschamps and Trampert, 2003; Mosca et al., 2012; Trampert et al., 2004; Trampert et al., 2001).

Density structure of the lowermost mantle can be inferred directly from tomographic studies that employ normal modes (also called free oscillations); however, density is not constrained as accurately as wave

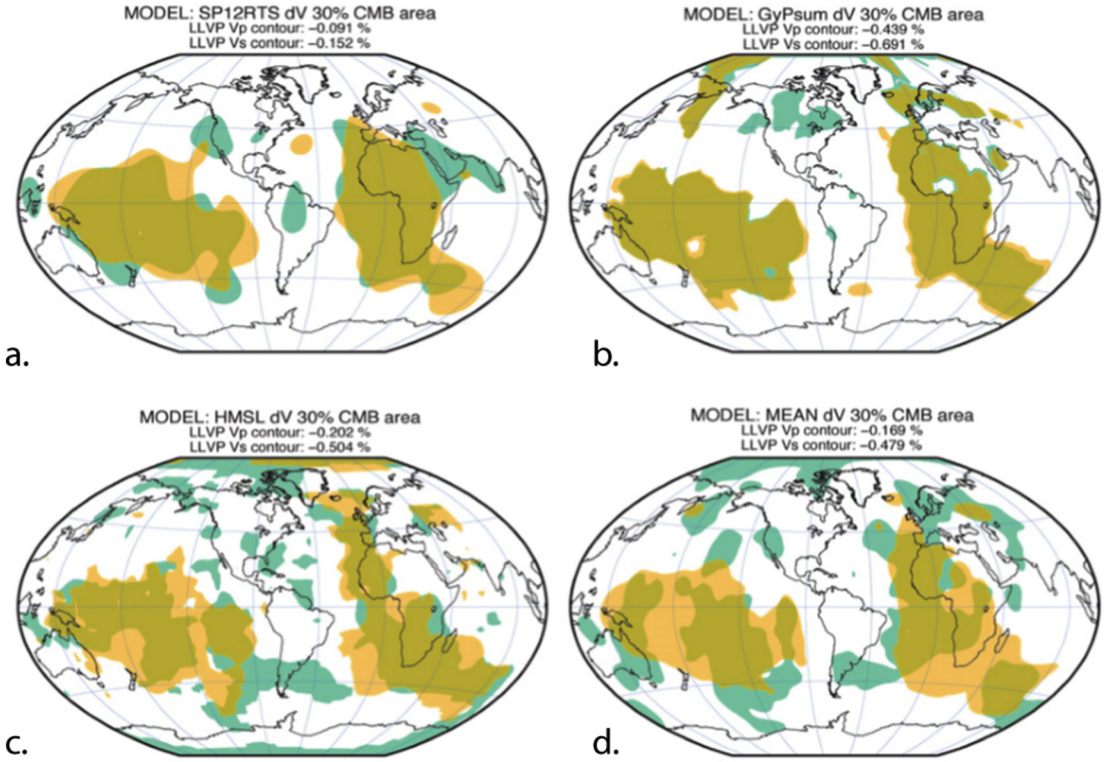

Fig. 4. Comparison of low velocity regions in compressional (P-wave) and shear (S-wave) joint tomography models.
Figure taken from Garnero et al. (2016), Supplementary Content. 30% core-mantle boundary area of lowest seismic velocities for S-waves (yellowish) and P-waves (green) in the lowermost mantle. **a.** Model SP12RTS (Koelemeijer et al., 2016). **b.** Model GyPsum (Simmons et al., 2010). **c.** Model HMSL (Houser et al., 2008) **d.** An averaging of models (Becker and Boschi, 2002). (For interpretation of the references to color in this figure legend, the reader is referred to the web version of this article.)

speeds are in these models (e.g., Lay and Garnero, 2011; Resovsky and Ritzwoller, 1999). Normal modes are oscillations that encompass the entire Earth, following a large earthquake. Such studies have yielded seemingly contradictory results. Earlier studies found that the lowermost mantle beneath Africa and the Pacific is characterized by higher-than-average density (Ishii and Tromp, 1999, 2001, 2004), whereas a recent study examining splitting of Stoneley modes (a type of free oscillation, most sensitive to lowermost mantle structure) found that observations are best fit if LLSVP regions exhibit lower-than-average density (Koelemeijer et al., 2017). However, Koelemeijer et al. (2017) point out that they cannot exclude the possibility of a high density base within the lower 100 km of the LLSVPs. From a dynamics standpoint (discussed later), it is not surprising to find LLSVPs having a net lower density (or at the very least, a complicated and highly-variable, small-scale density structure) regardless of which conceptual model is assumed for their cause. In contrast, Lau et al. (2017) used GPS measurements of body tide displacements and modeling to infer that the bottom two-thirds of LLSVPs are denser than the surrounding mantle by 0.5%. It is unclear if and how the two studies compare and contrast, given that they apply fundamentally different observations to density models that are relatively simple approximations to the complicated density heterogeneity that we actually expect for LLSVPs.

While seismic tomography provides the best view we have of the interior, it is a blurry and incomplete one at best (e.g., Bull et al., 2010; Bull et al., 2009; Ritsema et al., 2007; Schuberth et al., 2009). Tomographic studies cannot clearly delineate the LLSVPs from the surrounding mantle, nor can they clearly define LLSVPs as a source of compositional heterogeneity distinctly different from their surroundings. The most striking evidence that we have for LLSVPs being distinct from the surrounding mantle comes from travel-time and waveform seismic studies that infer sharp edges along their margins (e.g., Breger and Romanowicz, 1998; Ford et al., 2006; He and Wen, 2009, 2012; He et al., 2006; Ni and Helmberger, 2003a, 2003b, 2003c; Ni et al., 2005; Ni et al., 2002; Ritsema et al., 1997; Sun et al., 2007a; Sun et al., 2009; Sun et al., 2007b; To et al., 2005; Wang and Wen, 2004, 2007; Wen, 2001, 2002; Wen et al., 2001; Zhao et al., 2015). Here, “sharp” refers to strong gradients in elastic properties over length-scales of tens of kilometers (e.g., Ni et al., 2002). Such studies typically involve a wide array of seismic stations over a broad geographic area to record the wave energy generated from an earthquake. By comparing travel-times of the seismograms, one can differentiate sections of the fanned-out raypath array that contain anomalies (Fig. 5). The abruptness at which the change in travel-time occurs as one views across the spread of stations provides a measure of the sharpness of the anomaly. Of particularly utility is comparing the shape of the waveforms across stations. Ideally, after correcting for station and near-surface effects, the shape of a waveform should mostly depend on the source processes of the earthquake. However, as a portion of the seismic wavefront travels parallel to a sharp anomaly boundary (marked by a significant change in elastic properties), the part of the wavefront that travels inside the boundary will travel at a different speed than the part outside of the boundary. This results in stretching out the waveform, making it broader than it originally was. From these principles, hypothetical anomalies can be modeled and the resultant synthetic seismograms can be compared to observation to find the best fit anomaly model (e.g., He and Wen, 2009, 2012). A summary of sharp LLSVP edges from such travel-time and waveform studies is shown in Fig. 6. The first thing to note is that there are some contradictory results, particularly for sharp edges to the African LLSVP. This is not too surprising because the seismic models do not actually invert for shape; instead, they investigate multiple geometric structures and find which one best fits to observations, a procedure which provides a non-unique solution. However, knowing the exact geographic locations of sharp edges is not as valuable as knowing that a sharp edge exists, which is a robust result from these studies. It is

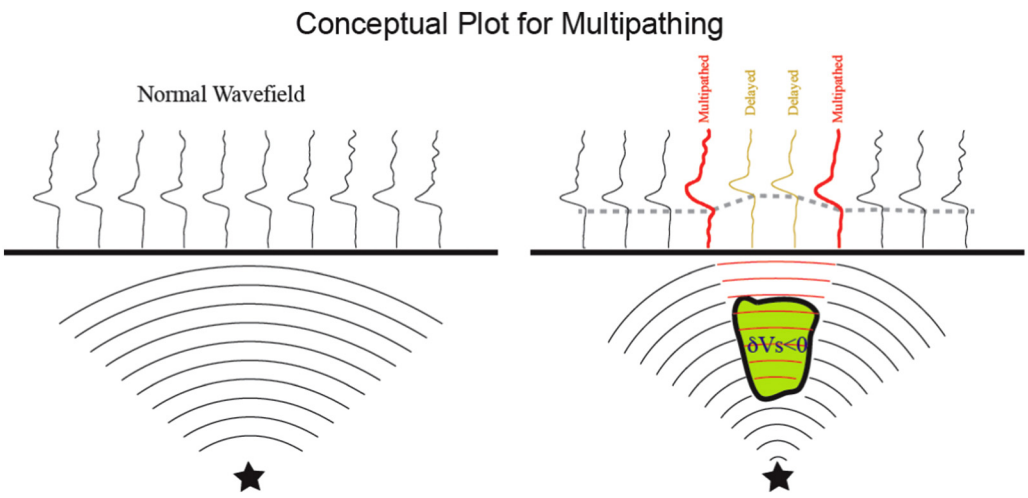

Fig. 5. Schematic example of waveform broadening due to sharp anomaly edges.
Figure provided and created by Chunpeng Zhao. Each figure shows an earthquake source (star), seismic wave fronts (semi-circles), and synthetic seismograms along an array at different azimuthal angles to the earthquake. **Left side**: In a situation without seismic anomalies, all seismograms have the same shape. **Right side**: The presence of an anomaly (yellow) both delays the seismic wave and broadens its waveform for the parts of the wave front that travels along the edges of the anomaly. (For interpretation of the references to color in this figure legend, the reader is referred to the web version of this article.)

interesting to note the sharp edges observed within the Pacific LLSVP (He and Wen, 2009), which is consistent with the seismic study of (Thorne et al., 2013) that infers a possible merging of smaller compositional anomalies there.

Sharp edges to the LLSVPs are typically considered evidence to support a compositional distinctness to them, in which the edge is a compositional boundary. This is largely because thermal diffusion is many orders of magnitude higher than chemical diffusion in the mantle, and therefore, it is traditionally-considered difficult for thermal anomalies to maintain strong gradients. However, geodynamics work demonstrates that purely thermal structures can also cause sharp gradients in elastic properties (Davies et al., 2012). Therefore, it important to note that a sharp edge only indicates a sharp change in elastic properties, and this can be achieved either compositionally, thermally or both. We expect compositional heterogeneity to cause sharp edges in general, and therefore it provides a strong candidate cause for them, but we can't exclude purely thermal possibilities that may develop in some cases.

2.2. Hotspots, ancient large igneous provinces, and past plate motions

Hotspots are regions on the Earth's surface marked by basaltic volcanism that is seemly unrelated to standard plate tectonic processes (e.g., Duncan and Richards, 1991). Hawaii and Yellowstone are typical examples, but there are many others (Fig. 7). While a small number of hotspots, such as Iceland and Ascension, appear on or near divergent plate boundaries, most are located within the interiors of plates. A long-standing hypothesis for the cause of hotspots is that they are the surface expression of mantle plumes, thermal instabilities arising from the deep mantle (e.g., Morgan, 1971). Unfortunately, although many seismic studies provide hints and glimpses of plumes, we do not yet have complete, incontrovertible evidence of their existence. (e.g., Bijwaard and Spakman, 1999; Boschi et al., 2007; Courtillot et al., 2003; French and Romanowicz, 2015; Montelli et al., 2004; Ritsema and Allen, 2003; Schmerr and Garnero, 2006; Schmerr et al., 2010; Shen et al., 1998; Shen et al., 2003; Wolfe et al., 1997; Wolfe et al., 2009; Wolfe et al., 2011; Yang et al., 2006). However, mantle plumes are theoretically predicted to exist based on fluid dynamical experiments, of which there is a long and rich history of geodynamical work (e.g., Albers and Christensen, 1996; Bercovici and Kelly, 1997; Cserepes et al., 2000; Davies and Davies, 2009; Davies, 1990, 1995; Farnetani and Hofmann, 2009; Farnetani et al., 2012; Farnetani et al., 2002; Farnetani and Richards, 1994; Farnetani and Samuel, 2005; Farnetani and Richards, 1995; Gonnermann et al., 2004; Griffiths and Campbell, 1990; Jellinek et al., 2003; Jellinek and Manga, 2002, 2004; Kelly and Bercovici, 1997; Kumagai et al., 2007; Lassak et al., 2010; Li et al., 2014a; Lin and van Keken, 2005, 2006; Lowman et al., 2004; McNamara and Zhong, 2004; Mittelstaedt and Tackley, 2006; Ribe and Christensen, 1994; Richards et al., 1989; Richards et al., 1991; Samuel and Farnetani, 2003; Schubert et al., 1995; Schubert et al., 2004; Sleep, 1990, 2006; Sleep et al., 1988; Steinberger, 2000; Steinberger et al., 2004; Tan et al., 2002; van Keken, 1997; van Keken and Gable, 1995; Zhong, 2006; Zhong and Hager, 2003; Zhong and Watts, 2002). Historically, mantle plumes were hypothesized to originate from a thermal boundary layer at the core-mantle boundary, but if LLSVPs are caused by compositional heterogeneity, plumes could instead originate from thermal boundary

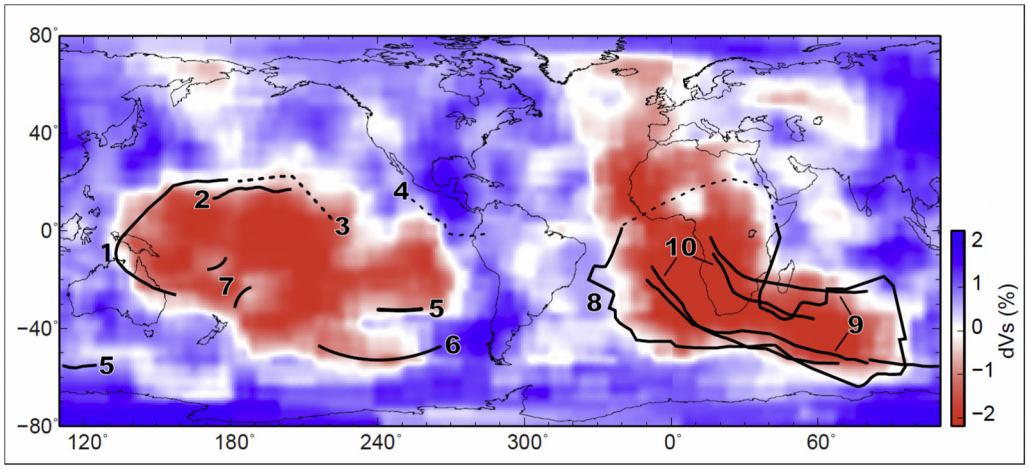

Fig. 6. Sharp edges inferred from seismic travel-time and waveform broadening studies.
Figure taken from Hernlund and McNamara (2015), created by Ed Garnero. The background color is shear-wave tomography from Grand (2002) in the lowermost mantle. Bold curves indicate sharp edges inferred from the following seismic studies: (1) He et al. (2006) (2) Luo et al. (2001) (3) Breger and Romanowicz (1998) (4) Sun et al. (2007b) (5) To et al. (2005) (6) Ford et al. (2006) (7) He and Wen (2009) (8) Wang and Wen (2004) (9) Sun et al. (2007a) and Sun et al. (2009) (10) (Ni and Helmberger, 2003a, 2003b, 2003c).

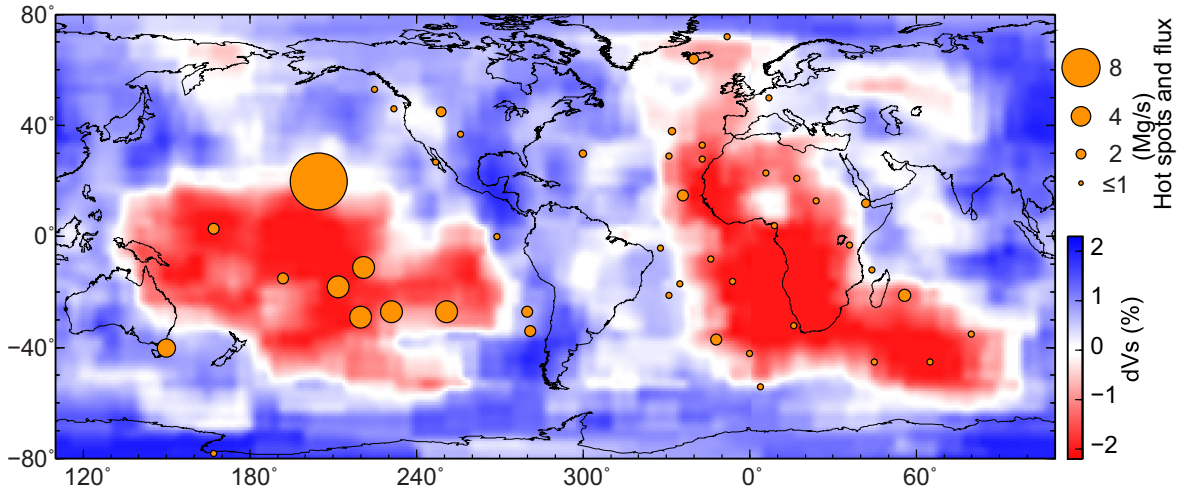

Fig. 7. Hotspots and LLSVPs.
Figure modified from Zhao et al. (2015). Background color map is shear-wave tomography of the lowermost mantle (2750 km depth) from Grand (2002). Orange circles represent hotspot locations, with radius of circle representing hot spot buoyancy flux (Sleep, 1990).

layers on the tops of LLSVPs (e.g., Davaille et al., 2002; Garnero and McNamara, 2008; Garnero et al., 2016; Hernlund and McNamara, 2015; Tackley, 1998; Tackley, 2012).

Upon examination, it is apparent that most (but not all) hotspots are located over the LLSVPs. This correlation motivates a hypothetical linkage between LLSVPs, mantle plumes, and surface hotspots, in which LLSVPs act as the source regions for most plumes. This notion is supported by recent seismic results. The tomographic model of French and Romanowicz (2015) integrates computationally-intensive forward wave modeling into the tomographic inversion process to provide a much more-detailed image of the mantle, illuminating LLSVPs that consist of much smaller-scale features than previous tomography models have shown and having more plume-like extensions that extend to the upper mantle, beneath various hotspots (Fig. 8).

The idea that mantle plumes are rooted from LLSVPs and cause hotspot volcanism at the surface is also “convenient” from a first-order geochemical perspective. Geochemical observations from Earth's surface have long hinted at the presence of multiple compositional reservoirs in the mantle (e.g., Albarede, 1998; Allegre, 1982; Allegre and Turcotte, 1986; Cabral et al., 2013; Carlson, 1994; Gonnermann and Mukhopadhyay, 2007, 2009; Graham, 2002; Hart, 1971; Hofmann, 1997; Jackson et al., 2014; Mukhopadhyay, 2012; Porcelli and Ballentine, 2002; Tackley, 2000; Tackley, 2007; Tolstikhin and Hofmann, 2005; Tolstikhin et al., 2006; White, 1985; White, 2015a, 2015b). The basalts formed at hotspots (named Ocean Island Basalts, or OIBs for short) have a different trace element chemistry than the basalts formed at mid ocean ridges (named Mid Ocean Ridge Basalts, or MORBs for short). Firstly, the trace element chemistry of OIBs is highly variable, both spatially (from hotspot to hotspot) and temporally (between basalts of different age within the same hotspot track). In contrast, MORBs have a relatively uniform trace element chemistry, globally. One type of trace element chemistry is incompatible elements, which are elements that preferentially go into the melt phase upon partial melting. MORBs are relatively depleted in incompatible elements, providing evidence that the mantle source rock has undergone previous melting in the past (expunging the incompatible elements at that earlier melting event). OIBs are less depleted, and sometime even enriched in incompatible elements, indicating that their source material has undergone less or no melting in the past, compared to MORBs (Fig. 9a). In addition, MORBs are more uniform in $^{3}He/^{4}He$, having a value that is typically about 8× larger than the atmospheric level. In contrast, OIBs have a much more variable $^{3}He/^{4}He$ ratio, again both spatially and temporally. OIBs also typically have a higher $^{3}He/^{4}He$ ratio than MORBs (Fig. 9b). Examination of additional trace element isotopic ratios (e.g., lead, neodymium, etc.) reveal 4–5 distinct chemical signatures within OIBs (i.e., EM1, EM2, HIMU, PREMA (also called FOZO), and putatively LOND) (Fig. 9c). White (2015a, 2015b) provide comprehensive and historical reviews. Consequently, it becomes an attractive hypothesis to surmise that LLSVPs are compositional reservoirs in the deep mantle that are tapped by mantle plumes that carry entrained LLSVP material to the surface, which then melts due to decompression melting to form hotspot lavas (e.g., Farnetani et al., 2012; Weis et al., 2011; Williams et al., 2015).

As stated above, most hotspots appear to overlie LLSVPs, but it appears that they may also be preferably located along LLSVP margins. Thorne et al. (2004) demonstrated that in the lowermost mantle, the margins of the LLSVPs are characterized by strong gradients in shear wave speed (in tomography models). They also found that hotspots are preferentially located above these strong gradients. In fact, they found hotspots are twice as likely to overlie LLSVP margins than their interiors. If one assumes that plumes rise vertically upward with only minimal deflection, this suggests that plumes are preferentially located along LLSVP margins. This preference for plumes to form along LLSVP margins has been observed in some geodynamical convection models that assume LLSVPs are caused by compositional heterogeneity (e.g., Steinberger and Torsvik, 2012; Tan et al., 2011), although this is not a typical feature of geodynamical calculations in general. In any case, it has been long known from dynamical models that plumes can be easily deflected by background convection currents (i.e., the “mantle wind”) (e.g., Steinberger, 2000; Steinberger et al., 2004), so it is unclear how confidently we can vertically project plume source in the lowermost mantle from the surface hotspot location. Nonetheless, the loose connection between hotspot locations and LLSVP margins is intriguing and warrants further investigation.

Burke and Torsvik (2004), Burke et al. (2008), Torsvik et al. (2008b), and Torsvik et al. (2010a) also recognized that most present-day hotspots are located above LLSVPs, and that there seems to be a preference toward them being located over LLSVP margins. However, they advanced this idea further by looking at the paleo-locations of large igneous provinces (LIPs) and kimberlites that erupted over the past few hundred million years. LIPs, also called flood basalts or traps, are massive accumulations of basalt (of a volume significantly greater than present-day hotspot volcanoes) that are hypothesized to be the result of plume head melting as a plume first reaches the surface (e.g., Richards et al., 1989). Using paleomagnetic plate reconstructions, they rotated the LIPs and kimberlites to their original eruption locations and

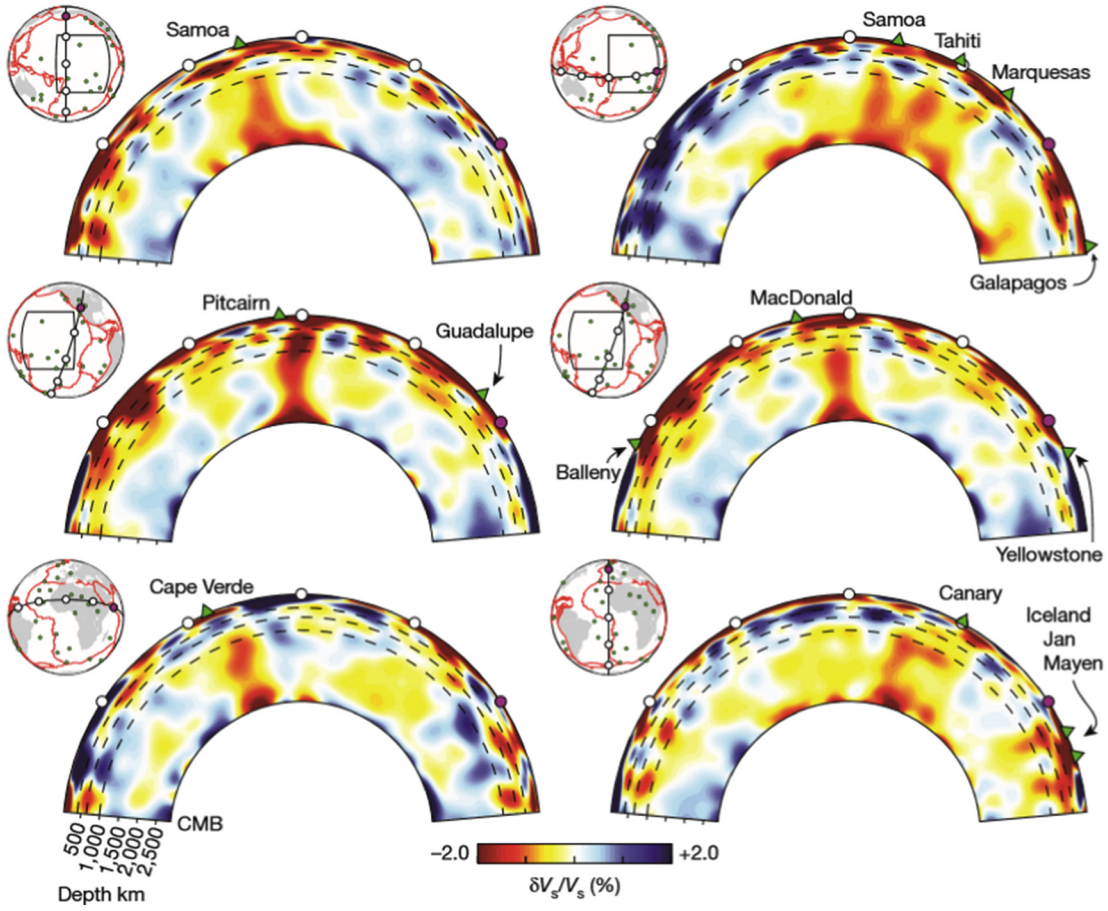

Fig. 8. Various cross sections of shear-wave tomography model SEMUCB-WM1.
Figure modified from French and Romanowicz (2015). Cross-section lines are shown in the globes to the upper-left of each cross-section. Green triangles mark particular hotspots at the surface. (For interpretation of the references to color in this figure legend, the reader is referred to the web version of this article.)

found that they coincide with the present-day locations of LLSVPs, with a preference toward present-day LLSVP margins (Fig. 10). This observation is potentially telling us something very important about the temporal stability of LLSVPs. However, in going forward, there are two levels of detail (or geographical resolution) to consider, depending on whether we correlate hotspots, past and present, with (1) the positions of LLSVPs in general or (2) the position of their geographic outline (i.e., LLSVP margins). It is unclear and debated whether the second is statistically significant (e.g., Austermann et al., 2014; Doubrovine et al., 2016). In either level of detail, if we assume that the correlation of present-day hotspot locations with present-day LLSVP locations (or their margins) is not coincidental and is based on some dynamical linkage (e.g., that plumes preferentially form above LLSVPs (or their margins)), then these results support the idea that LLSVPs (or their margins) have remained in their present-day position for several hundred million years.

The dynamical implications are significantly different for the two levels of detail we consider. If we assume that plumes preferentially form over LLSVP regions in general, these observations hint that LLSVPs have been roughly in the same locations as they are now for the past several hundred million years. This provides a valuable observational constraint on the lateral stability of deep mantle convection currents, which in turn provides critical information of lower mantle viscosity and global scale convection in general. Additionally, stability on the order of hundreds of millions of years is not unusual from fluid dynamical models (e.g., McNamara and Zhong, 2004). On the other hand, if we assume that both (1) plumes preferentially form over LLSVP margins and (2) ancient LIPs and kimberlites map to the same locations as present-day LLSVP margins, this implies a more-rigid stability of LLSVPs. Taken to an end-member tight mapping to present-day edges, it could indicate that not only have LLSVPs remained in the same locations over the past several hundred million years, but they haven't changed their shape in response to changing plate motions and subduction locations. This scenario would tell us something fundamentally new, important, and different about the long-term stability of mantle convection currents. The next important question would be whether LLSVPs (whatever they are) are the drivers of this stability or simply the consequence of it. In any case, such rigidity would be unconventional from a dynamical perspective, largely because past geodynamical work predicts LLSVPs (whether they are caused by thermal or compositional anomalies) should be easily and passively swept aside by changing downwelling patterns through time (e.g., Bower et al., 2013; Bull et al., 2009; Flament et al., 2017; Lassak et al., 2010; McNamara and Zhong, 2005; Zhang et al., 2010). However, most earlier geodynamics work has not investigated rheological scenarios that could potentially reduce how passive compositional anomalies are to time-dependent global convection currents. For example, McNamara and Zhong (2004) found that compositional anomalies with a higher intrinsic viscosity than background mantle could form strong, dome-like structures that don't appear to be deflected by downwellings. These domes were mobile, but the timescale of lateral motion was not compared to that of changing downwelling patterns, so it is unclear whether they were effectively stationary (meaning very slow) with respect to surface motions. More recently, Ballmer et al. (2017) investigated how differences in intrinsic viscosity due to variable SiO_2 content in the mantle can lead to the preservation of viscously strong, long-lived regions in the mantle

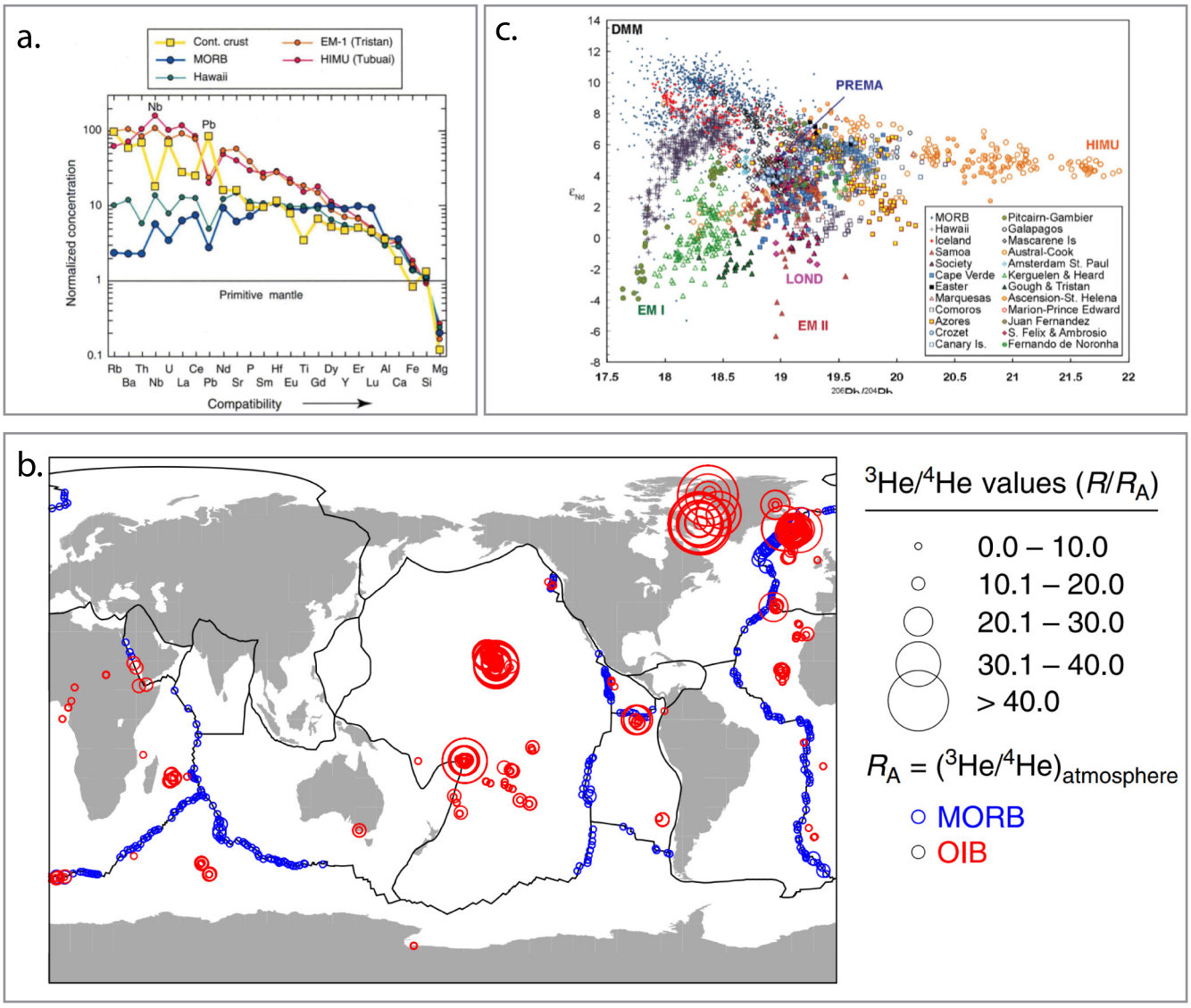

Fig. 9. Trace element geochemistry of MORBs and OIBs.
a. Concentration of incompatible elements as a function of compatibility for MORB, several OIBs, and continental crust. Taken from Hofmann (1997). **b.** Global distribution of 3He/4He ratios of MORBs (blue) and OIBs (red), relative to atmospheric values, RA. Compiled from the GEOROC, PetDB, and USGS noble gas databases. Taken from Williams et al. (2015). **c.** Nd versus Pb isotopic data from MORB and OIB, illustrating multiple, possibly independent compositional components. Taken from White (2015a). (For interpretation of the references to color in this figure legend, the reader is referred to the web version of this article.)

(named bridgmanite-enriched ancient mantle structures, or BEAMS for short) (Fig. 11). Furthermore, these BEAMS appear to have a stabilizing effect on mantle convection patterns. Future geodynamics work is needed to better investigate more-general intrinsic viscosity heterogeneities that are likely to exist in the mantle.

Conrad et al. (2013) performed a geodynamical calculation which used shear-wave tomography model S20RTS (Ritsema et al., 2004) to construct the density field, in order to model present-day, instantaneous flow patterns in the mantle. From these flow patterns, they computed the dipole and quadrupole convergence/divergence poles of the driving forces associated with slab pull and the basal tractions on the plates. Dipole and quadrupole components are related to degree-1 and degree-2 convergence and divergence. They then examined present-day plate motions (Demets et al., 1994) and extracted the dipole and quadrupole component poles from them and found that the poles match quite well to those from the convection calculation. This provides evidence, for the present-day at least, that plate motions and convection patterns share similar dipole and quadrupole divergence/convergence characteristics. However, it is unclear whether this dynamical linkage holds for all times in the past or whether it is a special case for the present day. Of particular interest to this study, both the convection model and the present-day plate motions agreed on quadrupole convergence beneath the western Pacific and South America and quadrupole divergence over the eastern edges of the LLSVPs. In particular, this shows that LLSVP regions are associated with an upwelling divergence of global flow that is reflected in overall plate motions. Next, they examined the dipole and quadrupole convergence/divergence poles for plate motions over the past 250 Ma (Seton et al., 2012; Steinberger and Torsvik, 2008; Torsvik et al., 2008a; Torsvik et al., 2010b). Interestingly, they found that the quadrupole divergence poles remained over the LLSVP regions for all times (Fig. 12). If the plate motion quadrupole divergence poles are indicative of quadrupole divergence in the mantle (as they have shown for present day plate motions), this provides evidence (although perhaps inconclusive) that mantle convection has retained a quadrupole divergence over LLSVPs, meaning that these regions have remained upwelling regions for several hundred million years. Combined with mapping the paleo-locations of LIPs and kimberlites, this provides additional evidence for LLSVP lateral stability

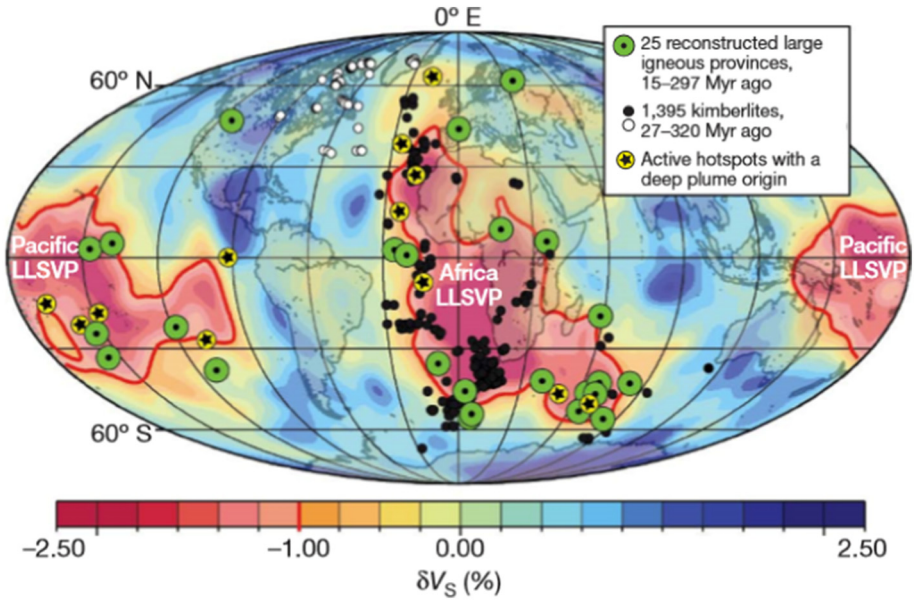

Fig. 10. Locations of present-day hotspots and paleolocations of ancient hotspots, large igneous provinces, and kimberlites.
Figure is taken from Torsvik et al. (2010a). Background color map is an average of shear-wave seismic tomography models at 2800 km depth, SMEAN (Becker and Boschi, 2002). The red line is a contour of −1% of velocity anomaly. Present-day hotspots with a suggested deep source are shown as yellow circles and stars. Paleolocations of large igneous provinces are shown as green circles with black dot inside. Paleolocations of kimberlites are shown as white and black circles. (For interpretation of the references to color in this figure legend, the reader is referred to the web version of this article.)

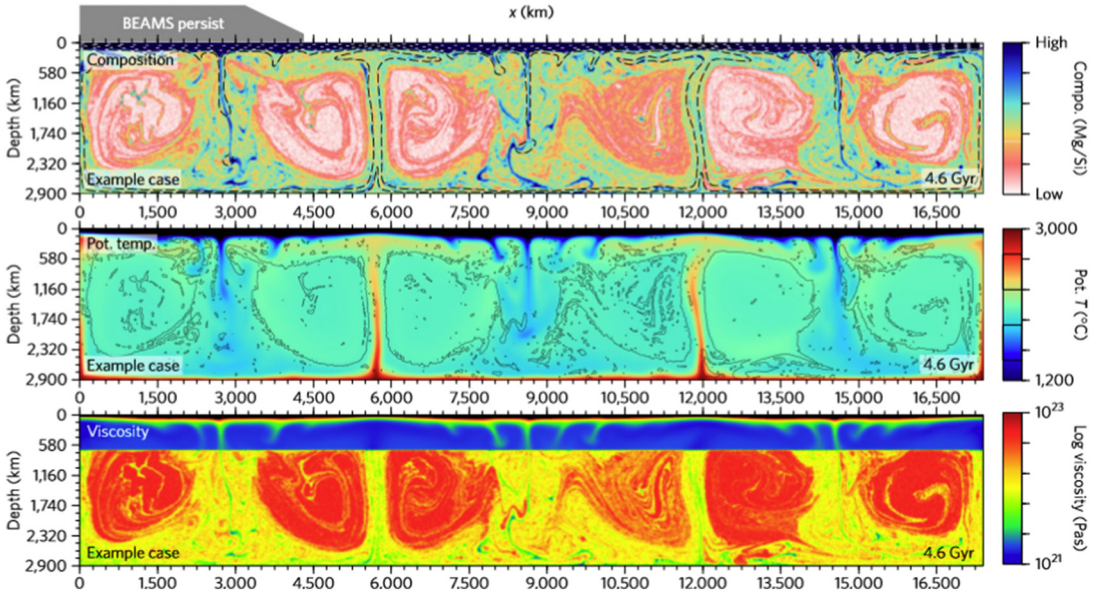

Fig. 11. Geodynamical calculation demonstrating how compositional rheology can stabilize mantle convection patterns.
Figure is modified from Ballmer et al. (2017). **Top-panel**: Compositional field, colored by Mg/Si ratio. Low Mg/Si ratio regions have a higher intrinsic viscosity. **Middle-panel**: Potential temperature field. **Bottom-panel**: Viscosity field. Note the high viscosity cores within convection cells, caused by lower Mg/Si ratio there.

over hundreds of millions of year.

If LLSVPs have indeed been stationary beneath Africa and the Pacific throughout the Phanerozoic, then they can provide a powerful tool to constrain paleolongitude of the plates (e.g., Torsvik et al., 2010a; Torsvik et al., 2014). For the past 100–200 million years, plate motions through time can be directly determined by magnetic anomalies on the sea floor (e.g., Scotese et al., 1988; Seton et al., 2012). Obviously, the ability to use sea floor anomalies decreases as one goes back in time because the amount of sea floor to work with decreases. Beyond that, paleomagnetism of continental rocks can provide a paleolatitude and an angular orientation with respect to the pole, but due to the symmetry of the mostly-dipole magnetic field, the paleolongitude cannot be obtained. In many cases, geology can then be used to determine whether cratons were juxtaposed to each other, but the degree of freedom (in longitude) significantly impedes our ability to reconstruct plate motions throughout the Paleozoic and early Mesozoic. However, if we could assume that LLSVPs are fixed (or even if they are relatively slow moving with respect to tectonic plates) and if we assume that most hotspots, LIPs, and kimberlites overlie them, then we have a mechanism to pin cratons that contain these volcanic features to a longitudinal range. Of course, if LLSVPs are completely fixed and plumes only rise from their edges, this would make the mechanism to determine paleolongitude more robust. However, even if we relax that assumption such that LLSVPs are not fixed but are slow moving with respect to plates and plumes may be formed anywhere above them (not just at their edges), this still provides a powerful means, albeit with more uncertainty, to constrain paleolongitude. In any case, it is the best (and perhaps only) tool we have at our disposal to reconstruct global plate motions beyond 200 Ma.

3. Hypothesized causes of LLSVPs

We don't know what the LLSVPs are, but we have several competing, candidate hypotheses to explain them. The main observations to

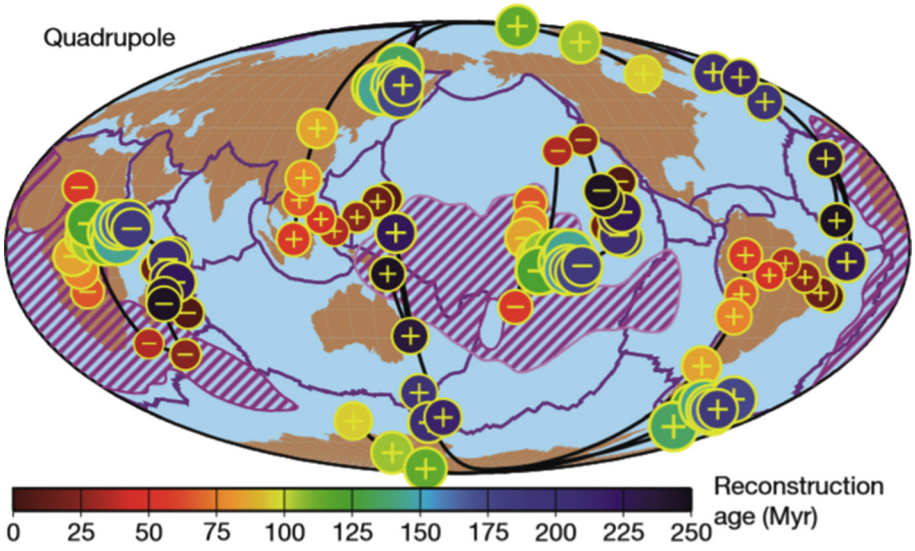

Fig. 12. Quadrupole locations of numerous plate reconstructions, spanning the past 250 million years. Figure modified from Conrad et al. (2013). Background global map displays present-day plate boundaries (dark purple) and the present-day location of LLSVPs (striped purple regions). Superimposed are quadrupole locations from plate reconstructions of various ages, displayed as colored circles, with color representing age of the reconstruction as noted on the color bar. Plusses represent quadrupole convergence, and minuses represent quadrupole divergence. The main aspect to point out is the persistence of quadrupole divergence over the LLSVPs over the past 250 million years, inferring stable locations of upwelling. (For interpretation of the references to color in this figure legend, the reader is referred to the web version of this article.)

satisfy are the sharp edges (in elastic properties), the anti- or non-correlation between shear-wave and bulk sound velocities, and the presence of numerous hotspots above them (which could be expressed as mantle plumes stemming from them). We expect that their density would not be too different from the surrounding mantle, but whether they are more or less dense is unclear. It would be convenient, although not strictly necessary, to relate LLSVPs to chemical heterogeneity, to explain the differences in trace element chemistry between OIBs and MORBs. At this time, it is perhaps too early to pose LLSVP stability over hundreds of millions of years as a constraint on hypotheses, but it is something that should surely be noted.

One can loosely categorize hypotheses for the cause of LLSVPs; however, note that these are mostly end-member scenarios and reality likely falls somewhere on the spectrum between them. At the top level, we can divide hypotheses between (1) thermal (or effectively isochemical) and (2) thermochemical. Effectively isochemical means that convection is driven solely by thermal buoyancy, and although compositional heterogeneity is not excluded, it does not provide a driving force for convection. Thermal models for LLSVPs can then be further divided into megaplume and plume cluster end-members. Thermochemical means that both thermal and compositional buoyancy drive convection, leading to a rich variety of dynamical possibilities. These hypotheses posit that LLSVPs are compositionally-distinct from the surrounding mantle, and they can be further categorized based on their time-averaged buoyancy and how much they stirred with the surrounding mantle. Following is an outline of categories for the cause of LLSVPs:

1) Thermal (or effectively isochemical)
   a) Megaplumes
   b) Plume clusters
2) Thermochemical
   a) Primordial (i.e., formed early)
      i) Domes and thermochemical superplumes (active, rising and sinking structures)
      ii) Primordial thermochemical piles (passive, negatively buoyant structures)
   b) Crustal accumulation (continually being created and destroyed)

Note that the above categorization is not unique, but it attempts to divide hypotheses into categories having fundamentally different consequences for long term thermal and chemical transport in the mantle. Furthermore, these are end-members with a wide spectrum of valid possibilities between them.

3.1. Thermal hypotheses for the cause of LLSVPs

By definition, LLSVPs are the lower-than-average regions of shear-wave velocity in the lower mantle. The most obvious cause of low shear-wave velocities is increased temperature; therefore, the most straightforward hypothesis is that LLSVPs are caused by large megaplumes of upwelling mantle. However, most geodynamical studies predict that hot regions, because of their lowered viscosity, are expected to form thin, narrow plumes (e.g., Campbell and Griffiths, 1990; Campbell et al., 1989; Griffiths and Campbell, 1990; Olson et al., 1993; Schubert et al., 2004; van Keken, 1997). However, some geodynamical studies have found the formation of large megaplumes when using high temperature dependent viscosity (Thompson and Tackley, 1998) or high thermal conductivity in the lowermost mantle (Matyska et al., 1994), but it is unclear whether megaplume formation could be a continuous process versus a “one-time event” in these cases. Because of the difficulty of demonstrating (in geodynamical models) the feasibility that megaplumes could exist over long geologic timescales, they are generally not discussed as a satisfactory hypothesis for the cause of LLSVPs. However, there is no ironclad evidence to exclude their possibility.

If LLSVPs are caused by thermal anomalies, it is more likely that they could simply be the blurred images of smaller plumes. This idea was first proposed by Schubert et al. (2004) and later demonstrated in geodynamical studies that employed tomographic “filtering” (e.g., Bull et al., 2010; Bull et al., 2009; Davies et al., 2012; Ritsema et al., 2007; Schuberth et al., 2009). The global convective mantle flow field, driven by subducting slabs, predicts that the African and Pacific parts of the mantle should exhibit lateral convergence and general upwelling flow (e.g., Bunge et al., 1998; McNamara and Zhong, 2005), and any mantle plumes that develop are expected to be focused there. Incomplete and heterogeneous raypath coverage (caused by the uneven and sparse distribution of both earthquake sources and seismic stations) causes seismic tomography to produce a blurred and distorted image of the deep interior. This is exacerbated by the damping and smoothing that occurs in the tomographic inversion itself. Therefore, it is possible that large seismic structures, such as the LLSVPs, may actually be the blurred images of smaller anomalies. Bull et al. (2009) explored this idea by performing isochemical geodynamical calculations, using the past 120 million years of plate motions (Lithgow-Bertelloni and Richards, 1998) to guide the formation of downwellings in the proper paleo-locations of subduction zones throughout that time. This resulted in the formation of clusters of plumes beneath Africa and the Pacific. They then applied a tomographic filter (from tomography models

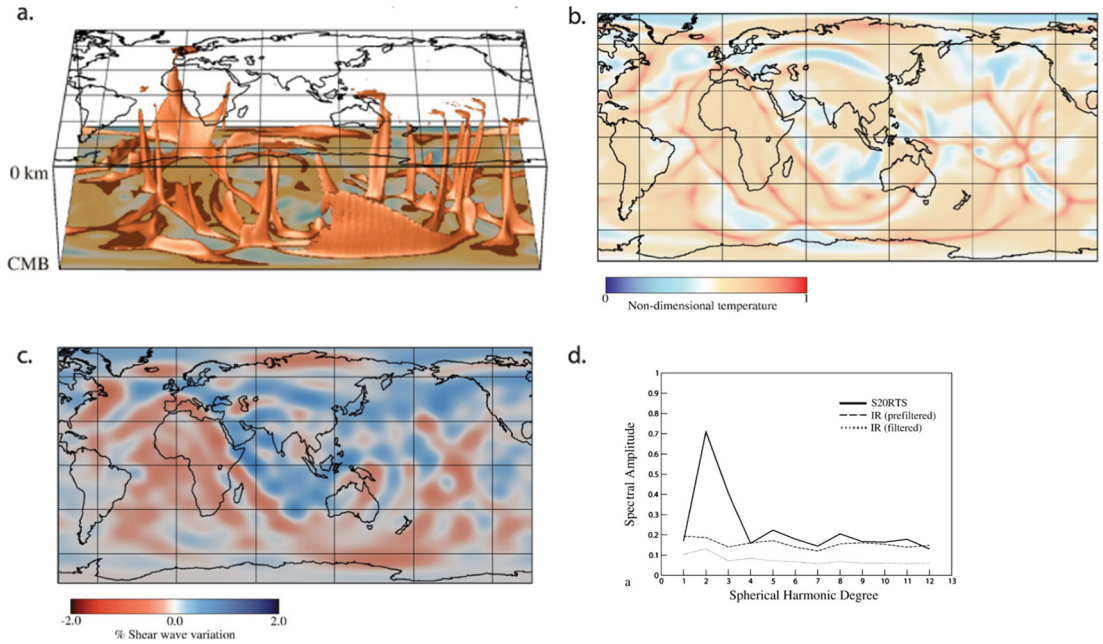

Fig. 13. Plume clusters and tomographic filtering of them.
Figure taken from Hernlund and McNamara (2015), which was modified from Bull et al. (2009). **a.** Isocontours (red) of hotter-than-average temperatures, outlining the locations of mantle plumes. These results are from a 3D spherical mantle convection calculation that employed the past 120 million years of plate motions at the surface to guide the locations of subduction. Spherical results are unwrapped unto a Cartesian box. Note the clustering of plumes beneath the African and Pacific regions. **b.** Temperature map about 150 km above the core-mantle boundary, illustrating the base of plumes. **c.** Map view of the synthetic tomography generated by tomographic filtering of the temperature field shown in panel b. **d.** Amplitude versus spherical harmonic degree at 2750 km depth of the S20RTS tomography model (Ritsema et al., 1999, 2004) (solid curve), temperature field from the geodynamical calculation (dark dashed line), and the synthetic tomography (light dashed line). (For interpretation of the references to color in this figure legend, the reader is referred to the web version of this article.)

S20RTS) to seismic velocities that were thermodynamically-derived from their temperature field (using Stixrude and Lithgow-Bertelloni (2005)) to blur it in the same manner that the tomographic inversion would. They found that tomography does indeed significantly blur thermal anomalies, making clusters of plumes appear as much larger objects (Fig. 13). Although their study concluded that the resultant filtered velocity field greatly enlarged thermal anomalies, the global power spectrum lacked the high power in low harmonic degrees that tomography exhibits. However, subsequent studies found much better agreement to tomography (e.g., Davies et al., 2012; Schuberth et al., 2009).

3.2. Thermochemical hypotheses for the cause of LLSVPs

There are several reasons that it is attractive to consider LLSVPs to be caused by a composition different from the surrounding, background mantle. Firstly, it provides a simple mechanism to explain the geochemical observations at the surface (described earlier). If the LLSVPs can act as geochemical reservoirs, it may help explain the difference in MORB and OIB trace element chemistry. To first-order, mid ocean ridges sample the background mantle to generate MORBs, whereas mantle plumes tap entrained reservoir material (i.e., LLSVPs) at depth and bring them to the surface to form OIBs (Fig. 14). Of course, this simple geodynamical-geochemical story is simply a motivating factor, not actual evidence. Therefore, the primary evidence pointing toward LLSVPs being compositional in nature comes from the sharp contrasts in elastic properties observed along their margins and the anti- or non-correlation between bulk sound speed and shear wave velocities, as described earlier. However, as convincing as these observations are, they are not particularly strong enough to provide a conclusive constraint for thermochemical over thermal models. In fact, Davies et al. (2012) demonstrate that thermal models can do an equally good or perhaps better job at satisfying them.

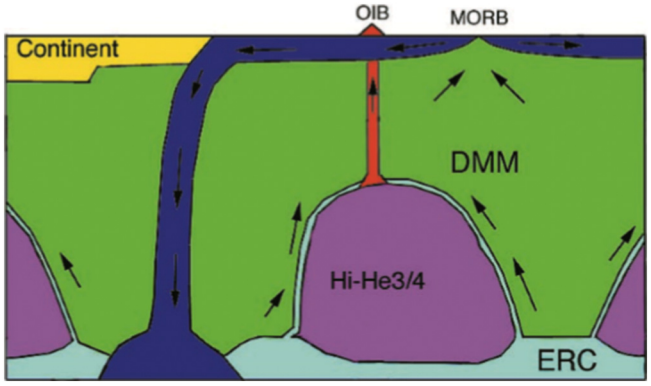

Fig. 14. Cartoon model of compositional reservoirs in the lower mantle and possible relationship to geochemical observations of MORBs and OIBs.
Modified from Tackley (2000). Purple and light blue regions represent lower mantle compositional reservoirs composed of more-primitive, high $^{3}He/^{4}He$ material and enriched recycled crust, respectively. Green represents depleted mantle material which is the source for MORBs. Dark blue represents subducting slabs, and red represents a thermal plume, tapping the compositional reservoirs and bringing some of that material to the surface to form OIBs. (For interpretation of the references to color in this figure legend, the reader is referred to the web version of this article.)

The simplest thermochemical model we can envision is the presence of an ancient compositional reservoir that is clearly distinct from the surrounding mantle. The compositional reservoir would need to be intrinsically more-dense than the surrounding mantle to prevent wholesale stirring within the mantle by mantle convection. There are several hypotheses regarding the cause of this ancient reservoir, including remnants of a basal magma ocean (Labrosse et al., 2007), accumulation of dense melts created early during Earth's history (Lee et al., 2010; Nomura et al., 2011), accumulation of crust formed on the

very early Earth (Tolstikhin and Hofmann, 2005; Tolstikhin et al., 2006), and/or all of the above in what has been referred to as a "basal mélange" (Tackley, 2012). A commonality between these hypotheses is that they all invoke differentiation processes that occurred very early in Earth's history and resulted in a well-defined and delineated basal layer, which is why this type of model is often referred to as "primordial," which should be thought of as a physical term (not strictly chemical) in this regard.

Perhaps one reason that primordial thermochemical models have gained much attention over the years is because it is the most straightforward to investigate geodynamically; one initiates the model as a layered system (with the more-dense layer on the bottom) and investigates the resultant dynamics as a function of the volume and density of the more-dense layer and the material parameters employed throughout the system. Starting with Tackley (1998) and Davaille (1999), there has been a rich history of geodynamical modeling LLSVPs as primordial compositional reservoirs (e.g., Bower et al., 2013; Bull et al., 2009; Davaille, 1999; Davaille et al., 2003; Davaille et al., 2005; Deschamps et al., 2011; Deschamps and Tackley, 2008, 2009; Flament et al., 2017; Jellinek and Manga, 2002, 2004; Lassak et al., 2010; Lassak et al., 2007; Le Bars and Davaille, 2004; Li et al., 2014a; Li et al., 2017; Li et al., 2016; Li et al., 2014b; Li et al., 2015; McNamara et al., 2010; McNamara and Zhong, 2004, 2005; Nakagawa and Tackley, 2004; Ni et al., 2002; Tackley, 2002; Tan and Gurnis, 2005, 2007; Tan et al., 2011; Zhang and Zhong, 2011; Zhang et al., 2010). One key outcome from these studies is that the more-dense reservoir may take on different styles of dynamic morphology, largely depending on the reservoir volume and intrinsic density contrast compared to the surrounding mantle (e.g., Le Bars and Davaille, 2004). Rayleigh number and temperature-dependence of rheology play secondary, but still significant, roles as well. For a given reservoir volume, if the intrinsic density increase compared to background mantle is too small, the reservoir will get quickly stirred into global scale mantle currents and therefore destroyed in short order. If the intrinsic density of the reservoir is too high, it will simply form a stable, flat layer in the lowermost mantle. Only for intermediate intrinsic density increases (on the order of a few percent over that of background mantle) will the reservoir form a significant amount of topographic relief to it.

At this point, it is useful to differentiate between "intrinsic" and "effective" density contrast of the reservoir with the background mantle. Intrinsic density contrast refers to the difference in density between the reservoir and background mantle under the same temperature and pressure conditions. However, in thermochemical convection, the more-dense reservoir always becomes significantly hotter than the background mantle, effectively reducing its density due to thermal expansion. Therefore, in thermochemical models that result in dynamic structures (not a layer nor quickly stirred into the mantle), the effective density of the reservoirs is very similar to that of the background mantle; in other words, they are near-neutrally buoyant. This is apparent in studies that display the buoyancy structure, revealing a complex distribution of both positive and negative buoyancy within different parts of the reservoirs (e.g., Lassak et al., 2007; Tan and Gurnis, 2005, 2007). Therefore, if LLSVPs are caused by compositional reservoirs, it is not surprising that seismic normal mode studies have mixed or unclear interpretations regarding LLSVP density, compared to background mantle (Ishii and Tromp, 1999, 2001, 2004; Koelemeijer et al., 2017).

For compositional reservoirs on the lower end of the intrinsic density spectrum, their overall, average effective density may become less than that of the background mantle, causing them to become temporarily buoyant. The reservoirs become dome- or plume-like and actively rise up through the mantle (e.g., Le Bars and Davaille, 2004) (Fig. 15a). These structures are typically referred to as "domes" and "thermochemical superplumes," and their positive buoyancy contributes momentum to global convection. Oftentimes, as they rise through the mantle, they cool enough to obtain an overall average negative buoyancy again and consequently sink back into the deep mantle, only to heat up again and repeat the cycle. These structures tend not to survive long geologic timescales as they are partially stirred into the mantle each time they rise and sink through it.

In contrast to the active domes and thermochemical superplumes, on the higher end of the intrinsic density spectrum, the overall effective density of the reservoirs remains slightly negative, leading to long-lived "piles" that remain on top the core-mantle boundary. These structures are commonly referred to as "primordial thermochemical piles" (Fig. 15b). Although they have a slightly-negative buoyancy, they weigh less than slabs (e.g., Lassak et al., 2010) and are therefore pushed away from subduction regions and are easily swept around by changing subduction patterns. They are shaped by mantle flow and accumulate along the core-mantle boundary directly beneath global upwelling regions (which for Earth, are the Pacific and Africa regions). Because of this, they are also coincident with thermal mantle plumes which are also pushed into these regions. Thermal mantle plumes are typically rooted along the tops of piles, forming narrow upward cusps in the pile-background mantle interface there via viscous stresses. At the plume roots, on top of the piles, pile material is entrained into plumes and to a lesser degree, background mantle is entrained into the piles adjacent to the plume (e.g., Deschamps et al., 2011; Li et al., 2014a; Williams et al., 2015). Under some conditions, plumes may form along the margins of piles instead of along their tops (e.g., Steinberger and Torsvik, 2012). Away from plumes, the pile-background mantle interface is clearly distinct with no mass exchange across it. Therefore, the only mass exchange that primordial thermochemical piles have with the background mantle is through the limited amount of entrainment at plume roots, the amount of which depends largely on the intrinsic density contrast between the piles and background mantle, but also the viscosity contrast between pile material and background mantle and the plume radius (e.g., Zhong and Hager, 2003). All thermochemical pile models are in a time-dependent state (they never reach equilibrium), in which the mass exchange at plume roots (albeit small in most cases) always acts to reduce the intrinsic contrast between piles and background mantle, which in turns increases the entrainment rates in a positive feedback process. Therefore, piles are always getting smaller in size, and their longevity may range from millions to many billions of years, largely depending on the initial intrinsic density contrast and viscosity contrast at the interface. Furthermore, primordial thermochemical piles heat up from the decay of radioactive elements and thermal conduction from the core below. Because heat escape from them is limited by thermal conduction out of their no-mass-flow interface, primordial thermochemical piles are always much hotter than the background mantle, often only slightly cooler than the core-mantle boundary itself.

Another style of thermochemical convection is characterized by compositional heterogeneity accumulating over geologic timescales. The primary mechanism hypothesized for this is the accumulation of subducted oceanic crust (e.g., Christensen and Hofmann, 1994; Davies and Gurnis, 1986; Gurnis, 1986) (Hofmann and White, 1982), which is motivated by mineral physics studies that indicate that subducted basaltic crust should become denser than background mantle at lower mantle pressures (Hirose et al., 1999; Hirose et al., 2005; Ringwood and Irifune, 1988). This hypothesis has inspired a great deal of geodynamics work through the years (e.g., Ballmer et al., 2015; Brandenburg et al., 2008; Brandenburg and van Keken, 2007a, 2007b; Christensen and Hofmann, 1994; Davies, 2008; Farnetani and Samuel, 2003; Huang and Davies, 2007; Mulyukova et al., 2015; Nakagawa and Buffett, 2005; Nakagawa and Tackley, 2005, 2006, 2011; Nakagawa et al., 2010; Samuel and Farnetani, 2003; Tackley, 2011; Xie and Tackley, 2004a; Xie and Tackley, 2004b). In general, the process entails the slab package (basaltic crust and lithosphere) reaching the lowermost mantle, followed by the separation of crust from the lithosphere. The process of separating crust from the lithosphere is critical because without it, most of the crust would easily get viscously stirred into the background mantle (e.g., Li and McNamara, 2013; Li et al., 2014a);

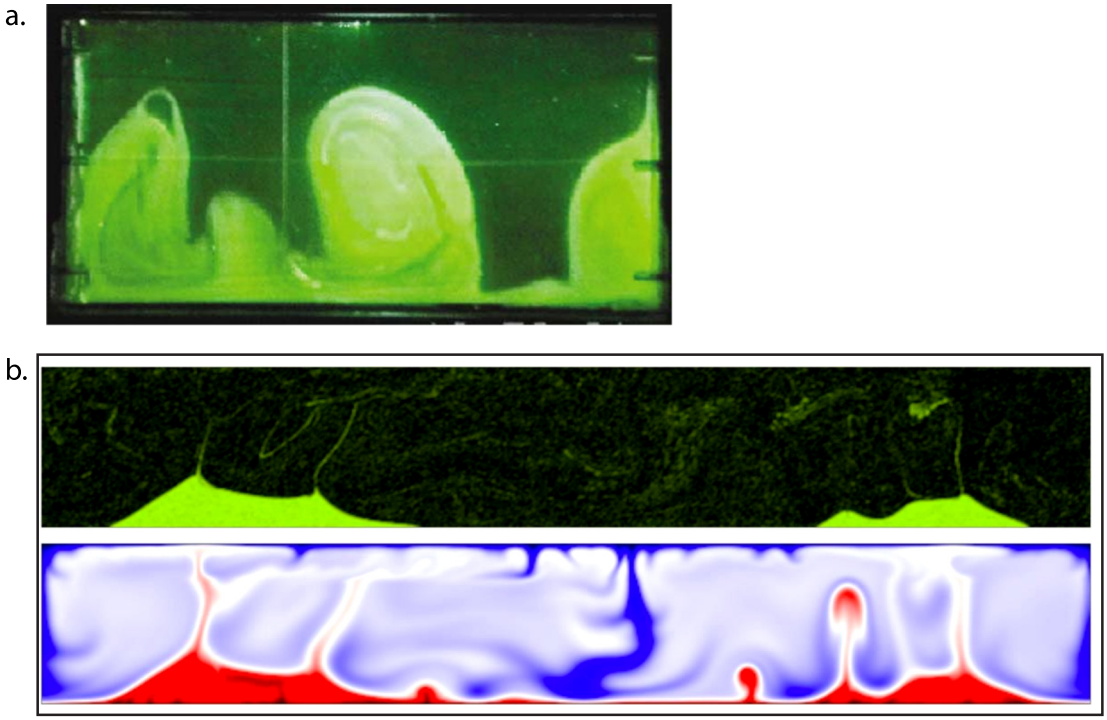

Fig. 15. Primordial thermochemical models of mantle convection.
a. Figure taken from Davaille et al. (2003). Results of a laboratory fluid dynamics experiment illustrating the development of thermochemical superplumes. An intrinsically dense layer (dyed with a florescent tracer) is temporarily more buoyant than the surrounding, after 3 cycles of rising and sinking through the tank. **b.** Snapshot from an unpublished geodynamical calculation performed by McNamara that leads to the formation of primordial thermochemical piles. The upper panel is the compositional field. Black represents background mantle and green represents intrinsically more-dense material. The lower panel shows the temperature field, with bluer and redder representing colder and hotter material, respectively. (For interpretation of the references to color in this figure legend, the reader is referred to the web version of this article.)

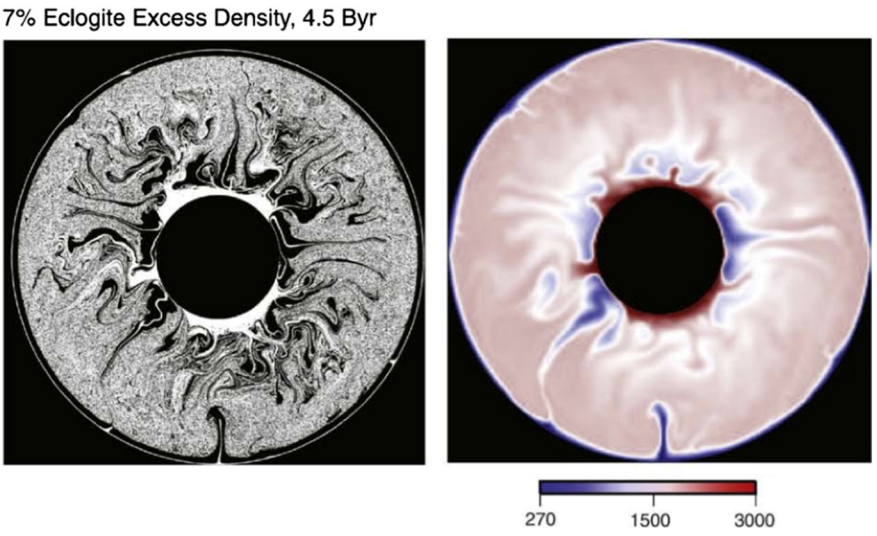

Fig. 16. Accumulated oceanic crust.
Figure modified from Brandenburg et al. (2008). Results of a thermochemical geodynamics calculation which employs a thin layer of basaltic crust (eclogite at higher pressure) at the surface that later accumulates in the lowermost mantle and also gets stirred into background mantle. In this case, the intrinsic density of crust is 7%, and the calculation is shown after 4.5 billion years. The left panel displays composition (crust is white, background mantle is black). The right panel displays the temperature field.

however, if post-perovskite is rheologically weak (e.g., Ammann et al., 2010; Hunt et al., 2012) segregation of crust from lithosphere is greatly enhanced (e.g., Li and McNamara, 2013; Li et al., 2014a; Nakagawa and Tackley, 2011). Once crust is separated from the lithosphere, it is then advected toward laterally convergent regions along the core-mantle boundary (which is the base of global upwelling regions). Stirring with background mantle is more prevalent in this kind of model, compared to the primordial models discussed above. As a result, the compositional fields in these models are visibly "messier" (Fig. 16). Even with efficient segregation of crust from lithosphere, a significant fraction of basaltic crust stirs into the background mantle. The heat and chemical transport within this type of thermochemical model is fundamentally different from the primordial models. In the primordial models, the compositional reservoirs have a clearly defined boundary with the surrounding background mantle, whereas in these models, material is always being advected into them from the sides and advected out through the top. Their margins are not well defined, and because of the mass flux into and out of them, heat is advected into and out of them as well (not limited to only conduction, like the primordial models). As a result, the mantle in these models tends to have less of a bimodal temperature structures than in primordial models that are characterized by very hot piles and a much cooler background mantle.

Modeling thermochemical convection due to crustal accumulation has historically had computational challenges and still retains some conceptual difficulties. The thinness of oceanic crust (~6 km) requires very high numerical mesh resolution, particularly in the lowermost mantle where segregation of crust from the lithosphere occurs, which was difficult to achieve until recently. Furthermore, it was difficult to model asymmetrical subduction; instead, fluid dynamical models typically produce double-sided, symmetrical subduction which led to oceanic crust being embedded within an envelope of higher viscosity, cold lithosphere once it entered into the mantle. Recent developments have made great strides toward resolving this issue (Crameri and Tackley, 2014; Crameri and Tackley, 2015; Crameri et al., 2012). Conceptually, we still have difficulty in that beyond several hundred million years ago, we don't have any evidence that subduction processes operated like they do today. For earlier times, we don't know the global extent of subduction (the total length of subduction zones), plate configurations and velocities, oceanic crust thicknesses, and whether plate tectonics operated as it does today. Therefore, it is difficult to approach this kind of modeling in an evolutionary context over geologic time.

Finally, it is quite possible that the Earth's mantle is experiencing multiple modes of thermochemical convection. We do know that oceanic crust descends into the mantle, although it remains under debate whether it can accumulate in the lowermost mantle to a significant extent (e.g., Li and McNamara, 2013; Mulyukova et al., 2015). The main question is whether ancient, primordial piles, domes, or superplumes exist. Several geodynamical studies have included both primordial reservoirs and accumulating oceanic crust, demonstrating a wide complexity of possible thermochemical dynamics and geochemical heterogeneity (Farnetani and Samuel, 2003; Li et al., 2014a; Nakagawa and Tackley, 2004; Samuel and Farnetani, 2003; Tackley, 2011) (Fig. 17). Geodynamical modeling can provide great insight into

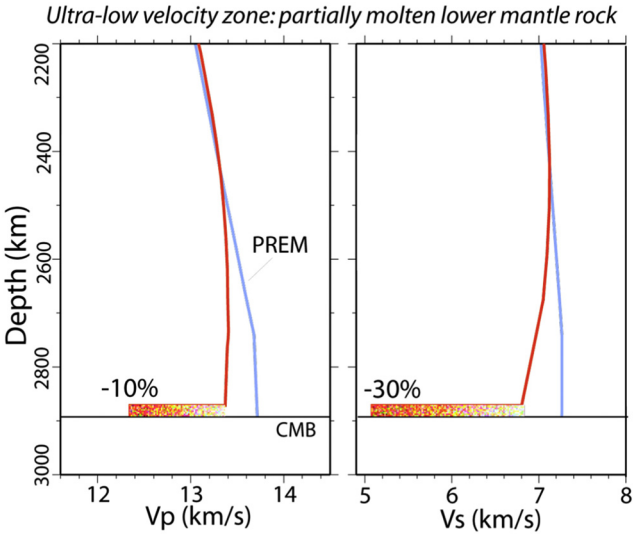

Fig. 18. Average seismic velocity reductions in Ultra Low Velocity Zones. Figure provided by Ed Garnero, colorized from Garnero et al. (1998). Left and right panels display average P- and S-wave velocities, respectively. The blue curves represent the global average (PREM). The red curves illustrate reductions in a typical ULVZ. Note that the red curves also include the 2–3% reduction inherent in the D″ layer within the lower couple hundred km of the mantle. (For interpretation of the references to color in this figure legend, the reader is referred to the web version of this article.)

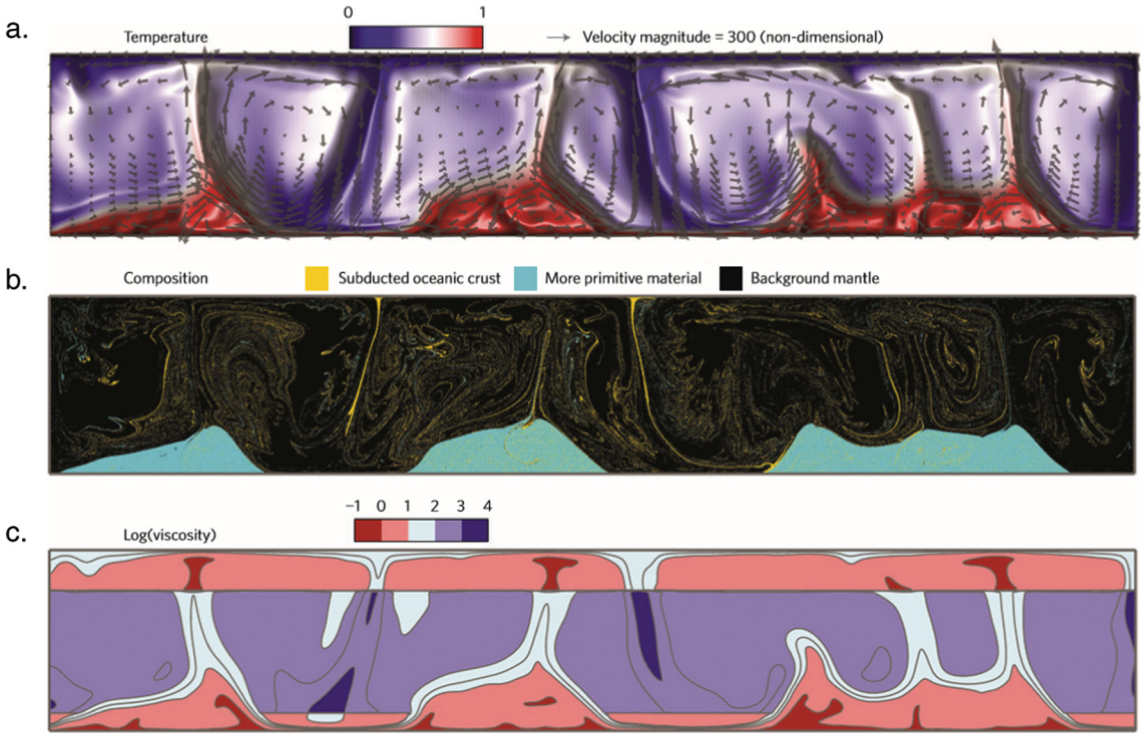

Fig. 17. Primordial thermochemical piles and subducted oceanic crust. Figure taken from Li et al. (2014a). Snapshot of a thermochemical geodynamics calculation of a three composition system: background mantle, primordial piles, and subducted oceanic crust. **a.** Temperature field with velocity vectors superimposed. **b.** Composition field showing background mantle (black), primordial piles (cyan), and subducted oceanic crust (yellow). **c.** Logarithm of non-dimensional viscosity, with contours marking every half-order-of-magnitude. The calculation employs a viscosity increase from upper mantle to lower mantle and a weakened post-perovskite at the base of downwelling regions. (For interpretation of the references to color in this figure legend, the reader is referred to the web version of this article.)

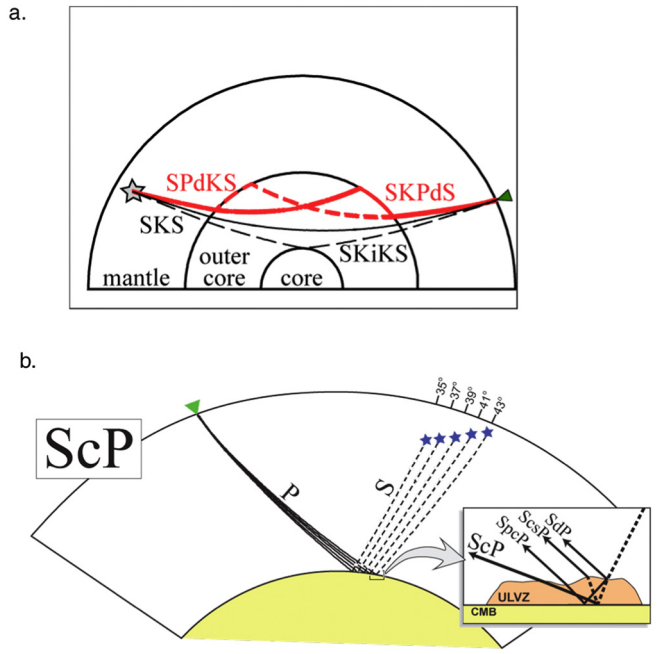

Fig. 19. Two different seismic methods to probe for ULVZs.
a. Modified from Thorne and Garnero (2004). Long-wavelength core diffracted waves, SPdKS and SKPdS in this example. **b.** Figure provided by Ed Garnero, colorized from Rost et al. (2006). Short-wavelength pre-cursors and post-cursors to core-reflected phases, ScP in this example.

the possible processes that may be occurring and can allow us to make predictions that can be tested by future seismic studies.

4. ULVZs

At a significantly smaller scale than the LLSVPs, Ultra Low Velocity Zones (ULVZs) are tiny patches on the core-mantle boundary that exhibit dramatic reductions of S- and P-wave velocity; up to 30% and 10%, respectively (e.g., Garnero and Helmberger, 1996; Garnero and McNamara, 2008; Garnero et al., 1998; Garnero et al., 2007; Williams and Garnero, 1996; Williams et al., 1998) (Fig. 18). ULVZs typically range from 10 to 40 km high and up to 100s of km laterally, with a couple notable exceptions of unusually more-laterally-expansive "mega ULVZs" extending up to 1000 km laterally (Cottaar and Romanowicz, 2012; Thorne et al., 2013). ULVZs are best modeled (seismically) as having large increases in density, up to 10% (e.g., Rost et al., 2005). ULVZs are not ubiquitous, and to the best of our understanding, they occur as disparate patches on the core-mantle boundary.

Much of the core-mantle boundary remains un-sampled with respect to ULVZs. There are several seismic methods used to detect ULVZs, each with different pros and cons. Long-wavelength waves diffracted along the core mantle boundary (for example, SPdKS and SKPdS) can provide wide ULVZ search areas (Fig. 19a). Although diffracted waves provide wide swaths of sampling area, they cannot geographically pinpoint ULVZ locations with any reasonable certainty, let alone provide any constraints on ULVZ size or shape. Instead, they can only provide information that reduced velocities are present somewhere along the swath. If ULVZ is detected, it is impossible to determine the number of individual ULVZs that may be present along the path. This is complicated by the mirror symmetry of the phases. For example, SPdKS and SKPdS (Fig. 19a) have identical travel times (for a given radial reference model), yet they each sample different sides of the core-mantle boundary. Therefore, it is unclear which side of the core the ULVZ detection is located, or whether there are ULVZs on both sides. However, if no ULVZ detection is indicated, it informs the observer that the mirrored swaths on both sides of the core are free of ULVZs. As a result of all this uncertainty, studies using diffracted waves typically present the results in terms of probability or "likelihoods" (e.g., Thorne and Garnero, 2004). A better way to locate ULVZs with high precision involves pre-cursors and post-cursors to core-reflected waves (e.g., Garnero and Vidale, 1999; Rost et al., 2006; Rost et al., 2005) (Fig. 19b). For a ULVZ located along the core-mantle boundary, a small fraction of the wave front energy is reflected off the top of the ULVZ before reflecting off the core, which shows up as a pre-cursor on stacked seismograms. Similarly, some energy from the core reflection will get reflected off the top of the ULVZ (from below), bounce back to the core and reflect again. This will show up as a post-cursor. By examining many nearby core reflection points by using an array of seismic stations, and correcting for near-surface structure, one can map out the size and shape of a particular ULVZ with great precision. The downside to this approach is that there is a very limited number of reflection points on the core-mantle boundary to interrogate, due to the sparse and heterogeneous distribution of earthquake sources and seismic stations. While this method provides excellent geographical resolution on

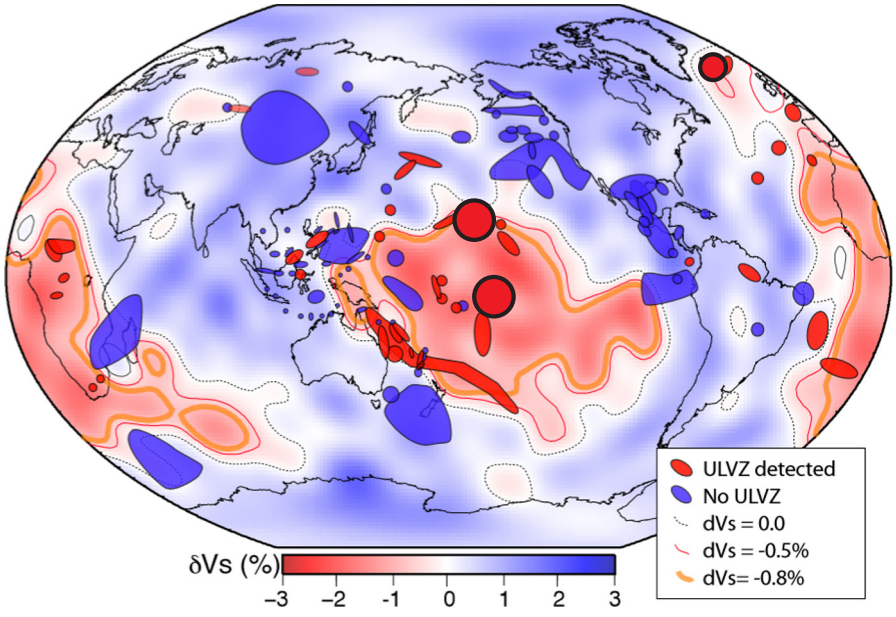

Fig. 20. Map of ULVZ detections and non-detections. Figure modified from McNamara et al. (2010). Background image is shear-wave tomography of the lowermost mantle, model S20RTS (Ritsema et al., 1999, 2004). Superimposed are dark patches correlated to seismic studies that search for ULVZs. Note that most of the mantle remains unmapped with respect to ULVZ. Dark blue patches represent regions interrogated and no ULVZ found. Dark red patches represent regions where ULVZ is found. Refer to McNamara et al. (2010) Supplementary Material for listing of seismic studies. Red circles with black outlines represent more recent ULVZ detections (Cottaar and Romanowicz, 2012; Thorne et al., 2013; Yuan and Romanowicz, 2017). (For interpretation of the references to color in this figure legend, the reader is referred to the web version of this article.)

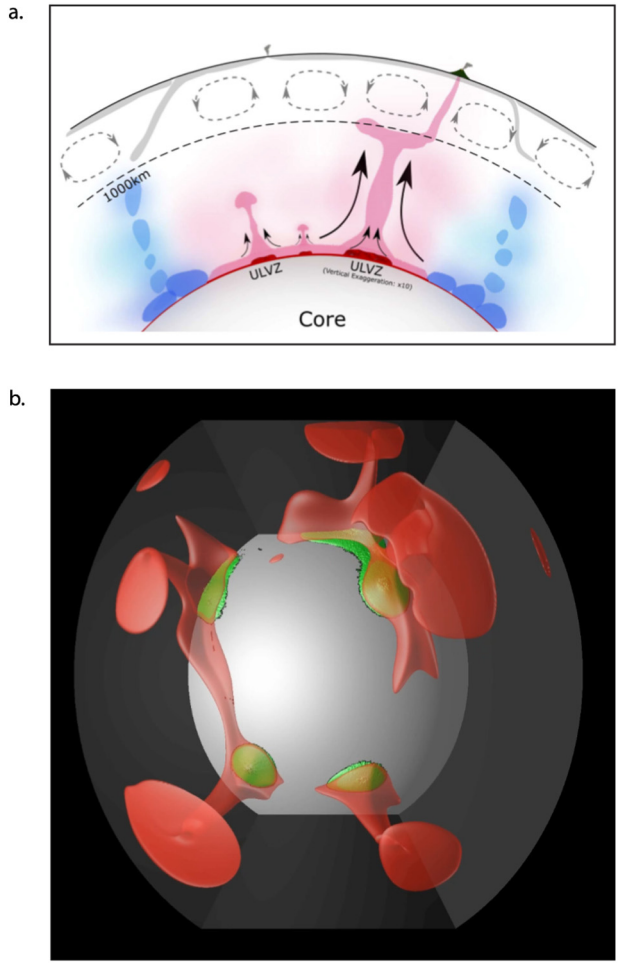

Fig. 21. ULVZs at the base of mantle plumes.
a. Figure taken from Yuan and Romanowicz (2017). Cartoon motivated by seismic observations of a ULVZ at the core-mantle boundary beneath Iceland. Combined with recent, high-resolution tomography results (French and Romanowicz, 2015), this ULVZ is interpreted to be a ULVZ at the base of a proposed Iceland mantle plume. **b.** Unpublished geodynamics calculation, performed by Mingming Li and related to research described in Li et al. (2017). The calculation was performed in a partial sphere 3D geometry. Gray marks the core-mantle boundary, and displayed in red are hotter-than-average isosurfaces that outline mantle plumes. A small volume of very dense material (green) naturally accumulates at the bases of the plumes. (For interpretation of the references to color in this figure legend, the reader is referred to the web version of this article.)

particular ULVZs, it does not provide much core-mantle boundary surface area to search. A more computationally intensive method to search for ULVZs involves waveform modeling (e.g., Cottaar and Romanowicz, 2012; Yuan and Romanowicz, 2017).

As discussed above, most of the core-mantle boundary remains unsampled. Fig. 20 provides a map, illustrating the sampled regions. The map background displays seismic tomography near the core-mantle boundary, and the geographic locations of numerous ULVZ studies are superimposed as dark blue and dark red patches. Dark blue and dark red represent sampled regions that indicate the absence or presence of ULVZ, respectively. One should use caution against overinterpreting the sizes and shapes of detections shown on the map; these are the result of different studies, with different methods, resolutions, and reliabilities. Furthermore, most ULVZ seismic modeling is one-dimensional, which can bias the estimates of height and width for the actual structures (which have a three-dimensional morphology). From looking at the image, it is easy to misread ULVZs as being “patches,” but note that these are study areas, not ULVZ shapes. Although some studies infer ULVZs to have a patch-like shape (e.g., Rost et al., 2005), this is not constrained by the majority of studies. Combined with the overwhelmingly large un-sampled area of core-mantle boundary, one should realize that our impression of ULVZ distribution is greatly compromised. The big question is, what does that un-sampled area look like? Is it mostly blue? Mostly red? Or is it a patchwork of both? If it is a patchwork, what is its typical length-scale? By imagining these different possible answers, one can get completely different outlooks on ULVZs and interpretations of their cause. For now, given the lack of information, most view ULVZs as patches, and many of our hypotheses regarding the cause of ULVZs somewhat assume this. But, we should use great caution with this assumption; clearly, more seismic studies need to be performed.

We don't know what causes ULVZs. Like with the LLSVPs, hypotheses can be loosely categorized as thermal (partial melt of hottest regions) and compositional (some ultra-dense material). These are idealized end-members that may not (in reality) exist in isolation because melting will change the composition and likewise, different compositions will have different melting temperatures. Nonetheless, they provide a good starting point for consideration. An early idea is that they are simply regions of partial melting in an otherwise normal mantle (e.g., Williams and Garnero, 1996). If this is the case, then we would expect them to exist in the hottest mantle regions. One difficulty with this idea is that dense melt would be expected to drain downward and form a melt-layer along the core-mantle boundary (e.g., Hernlund and Tackley, 2007). Perhaps there is such a ubiquitous melt-layer at the base of the mantle; if it is thin enough, it would be difficult to distinguish it from the liquid core. One can get around this difficulty, however, if ULVZs are assumed to be compositionally-different from the surrounding mantle. ULVZ material would then have a different melting temperature and not be constrained to exist in the hottest mantle regions. To survive viscous stirring into the surrounding mantle, it would need to have a significantly higher density (about 10% greater, consistent with observations) (e.g., McNamara et al., 2010). There are numerous hypotheses for the source of compositional ULVZs, including iron-enriched oxides (Bower et al., 2011; Wicks et al., 2017; Wicks et al., 2010), subducted banded iron formations (Dobson and Brodholt, 2005), silicate sediments from the core (Buffett et al., 2000), iron-enriched post-perovskite (Mao et al., 2006; Mao et al., 2005), melt within subducted oceanic crust (Andrault et al., 2014; Ohtani and Maeda, 2001; Pradhan et al., 2015), slab-derived metallic melt (Liu et al., 2016), and FeO_2 in pyrite structure (Hu et al., 2016).

Unlike the large-scale LLSVPs, ULVZs are so small that it's unlikely that they play a significant role in global mantle convection. However, it is likely that they are related to the LLSVPs in some dynamical sense, and therefore, the shape, sizes, and locations of ULVZs promise to provide valuable insight into the cause of LLSVPs and the nature of global convection. To best understand how ULVZs can be used to tell us about LLSVPs, we need to consider an IF/THEN approach. In a loose manner, we can consider the 4 end-member scenarios, each assuming either a thermal or a compositional cause for LLSVPs and ULVZs. **LLSVPs (thermal) and ULVZs (thermal)**: If we consider LLSVPs to be clusters of thermal plumes and ULVZs to be partial melt of an otherwise normal mantle, then it is clear that ULVZs would be located in the hottest regions of the lowermost mantle, which have been shown to be at the base of thermal mantle plumes (e.g., Bull et al., 2009). In this case, we'd expect ULVZs to have a relatively symmetrical shape (in cross-section) at the roots of plumes (or perhaps only at the hottest plumes). The recent seismic study of Yuan and Romanowicz (2017) located a ULVZ beneath the Iceland Hotspot, which they infer to be partial melt at the base of a plume (Fig. 21a). **LLSVPs (thermal) and ULVZs (compositional)**: If LLSVPs are clusters of thermal plumes, then the base of each one would be a region of localized convergent flow. If ULVZs are caused by an ultra-dense material, then we expect that material to accumulate at convergent regions, therefore, at the roots of

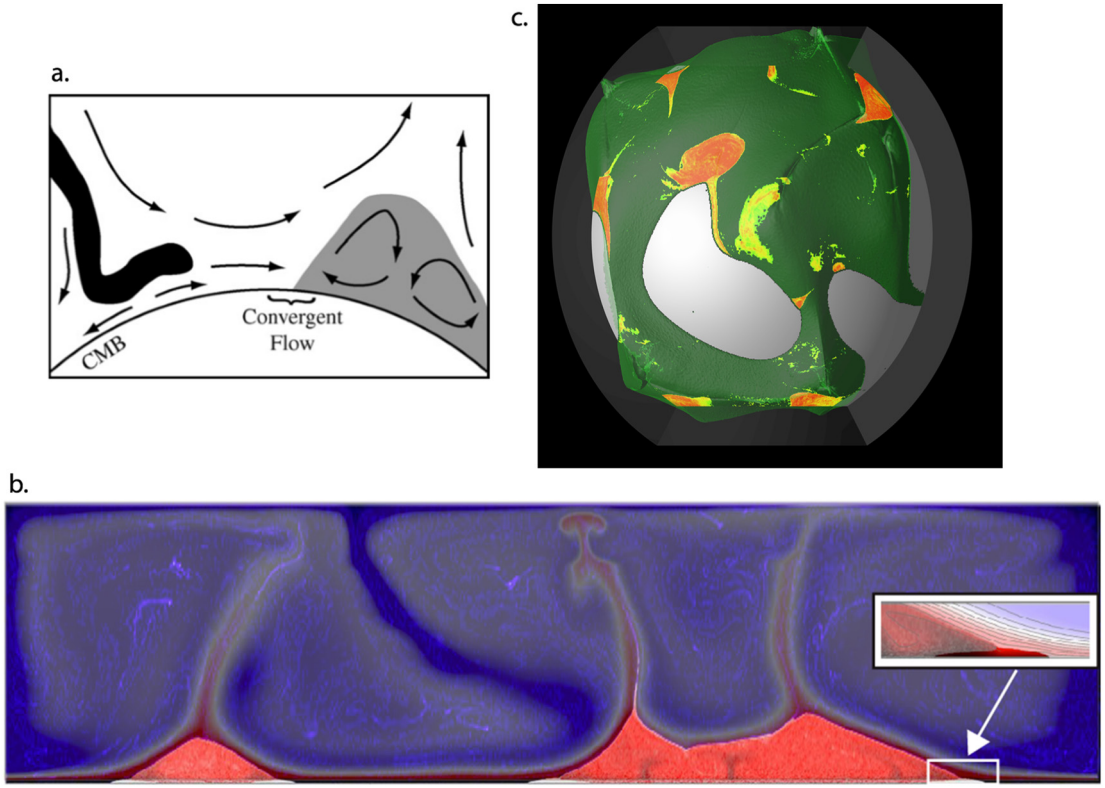

Fig. 22. Compositional ULVZs and LLSVPs.
a. Figure taken from Hernlund and Tackley (2007). Schematic diagram showing general nature of convective flow in a mantle that contains primordial thermochemical piles. The boundaries of piles are regions of convergent lateral flow. Any ultra-dense material in the lowermost mantle would accumulate in these regions. **b.** Thermochemical calculation containing primordial thermochemical piles and a small volume of ultra-dense material (hypothesized to cause ULVZs). The main image is a superposition of temperature and composition. Piles are marked by bright red and ultra-dense material is white. The inset shows a zoom-in at the base of a pile edge where convergent flow occurs. ULVZ is marked as dark red in the inset. This image is unpublished, but comes from work completed in McNamara et al. (2010). **c.** A similar thermochemical convection calculation, but performed in a 3D partial sphere geometry. The core is marked by gray. Primordial thermochemical piles are shown as semi-transparent green. Ultra-dense material in the lowermost mantle is shown by red-yellow color (visible through the green piles). Figure taken from Li et al. (2017). (For interpretation of the references to color in this figure legend, the reader is referred to the web version of this article.)

plumes (or at least the strongest plumes). The accumulations of ultra-dense material are expected to be relatively symmetrical in cross-section for an isolated plume (Fig. 21b). **LLSVPs (compositional) and ULVZs (thermal)**: If LLSVPs are primordial thermochemical piles, geodynamical studies consistently find that they are the hottest regions of the mantle, therefore, if ULVZs are thermal, they should exist within them. The recent geodynamical study of Li et al. (2017) found that the hottest regions within primordial thermochemical piles are well-inside their interior, far removed from pile edges. The shapes of the hottest regions are relatively symmetrical in cross-section view. Alternatively, if LLSVPs are accumulations of subducted oceanic crust, it is difficult to predict where the hottest regions would occur, and more work needs to be done to investigate this. **LLSVPs (compositional) and ULVZs (compositional)**: If LLSVPs are primordial thermochemical piles, the base of their margins would experience convergent lateral flow, and therefore any ultra-dense material would accumulate there (Fig. 22a). This has been observed in geodynamical calculations (e.g., Li et al., 2017; McNamara et al., 2010). Interestingly, geodynamical calculations reveal an asymmetrical shape to compositional ULVZs, thicker on the outside of the pile than on the inside (Fig. 22b). The reason for this is differential viscous stress on the ultra-dense material. The piles are much hotter than background mantle; therefore, they have a lower viscosity. Convection within the low viscosity pile cannot exert as much viscous stress on the ultra-dense material, compared to the higher viscosity background mantle. In other words, the background mantle on the outside of the pile can exert a stronger viscous force on the ULVZ, causing it to pile up higher there. The 3D geodynamical study of Li et al. (2017) reveals that accumulations of ultra-dense material are expected to form a patch-like distribution along the margins of primordial piles (Fig. 22b). Alternatively, if LLSVPs are accumulations of oceanic crust, then it is more difficult to generalize the locations of ultra-dense material, given the advective, messy nature of the fuzzy pile boundary. More geodynamical work needs to be performed to examine this.

In the above scenarios, it would be difficult to distinguish between the first three. Each would predict relatively symmetrically-shaped ULVZs throughout LLSVP regions. However, the asymmetry of ultra-dense material in the final possibility provides a powerful hypothesis test for future seismic studies. Such seismic studies would need to be performed in two- or three-dimensional geometry, unlike the bulk of previous studies that are performed in one dimension. Asymmetric ULVZs along LLSVP margins would strongly argue for the accumulation of ultra-dense material along the margins of a large compositional reservoir. Furthermore, ULVZs located outside of LLSVP regions are intriguing. Whatever LLSVPs are, we expect them to be the hottest regions of the lower mantle and areas of convergent lateral flow. Outside of LLSVPs, we expect temperatures to be cooler and flow to be directed toward LLSVPs. Therefore, it is attractive to consider ULVZs outside of LLSVPs to be compositional anomalies en route to LLSVPs. Perhaps they are chunks of oceanic crust (with partial melt due to lower melting temperature) that are in transit (e.g., Li et al., 2017), although this is highly speculative at this time.

5. Summary and future work

Discovering what the LLSVPs are is one of the most important problems that the deep Earth community is pursuing. The answer to that question will have profound implications for our understanding of global mantle convection, and therefore, our understanding of Earth's thermal and chemical evolution. It also has critical implications toward our understanding of MORB/OIB trace element chemistry, hotspots, and plate tectonic driving forces. Of particular recent interest is determining LLSVP stability over geologic time. Are LLSVPs simply passive features of mantle convection, or do they have a fundamental role in driving and stabilizing mantle flow patterns? Can they be used to provide a geographic reference point through time, providing a mechanism to constrain paleolongitude? To answer these questions will require continued additional observations from seismology. Each new seismic observation provides a small piece to that puzzle.

One target for future seismological investigation is to better image the tops of LLSVPs. Discerning sharp versus messy tops will provide key information on their cause. If LLSVPs are thermochemical piles, imaging their tops may allow us to distinguish between primordial piles and accumulations of oceanic crust. Furthermore, if LLSVPs are caused by clusters of plumes, they would have a very complicated, hard-to-define top. Better imaging interior LLSVP structure will provide many clues regarding whether LLSVPs are plumes or perhaps collections of smaller piles. In addition, the lowermost mantle remains mostly unexamined in terms of ULVZ presence. Because ULVZs may provide important clues to the cause of LLSVPs, continued hunting for them is critical, as well as developing new hunting methods to find them. ULVZs are typically modeled, seismically, as simple one-dimensional geometric structures, but by better discerning ULVZ shape, we can gain insight into their cause and relationship with LLVSPs.

On the geodynamics front, there is much that should be done regarding rheology. Most studies assume that thermochemical piles have the same rheology as background mantle. There is no reason to expect this to be the case, in general. For example, even if primordial piles and background mantle are composed of rheologically similar materials, there is no reason to expect that they should have the same mineralogical grain size, which greatly influences the magnitude of diffusion creep viscosity. Because we haven't explored alternative rheologies and/or grain-sizes for LLSVPs, we've only just begun to get a sense of the possible dynamical behaviors and resultant morphologies. New discoveries from mineral physics on how grain size evolves with pressure, temperature, and deformation history will be incredibly useful in this regard, although challenging to employ. Better understanding how polymineralic assemblages of mantle rock undergo deformation creep under different conditions is also needed. Furthermore, better understanding how multiple compositions (e.g., crust, primordial, ultra-dense ULVZ materials, etc.) interact together in a global mantle convection context has been greatly unexplored. Increased computational ability now allows us to model multi-scale compositional complexity at sufficient resolutions. Continued higher resolution seismic observations, combined with geodynamical modeling, will allow us to develop and test improved hypotheses regarding the cause of LLSVPs. Combined with new mineral physics results and geochemical observations, these will allow us to better understand the cause and significance LLSVPs and ULVZs.

Acknowledgements

This work was partially supported by the following NSF grants: EAR-1722623, EAR-1644453, and EAR-1664332. I thank Ed Garnero, Chunpeng Zhao, and Mingming Li for help with figures. This review benefited greatly by long discussions with Ed Garnero and Mingming Li. I would like to thank Philippe Agard, Bernhard Steinberger, and 2 anonymous reviewers. This paper is dedicated to Molly and Baxter.

References

Albarede, F., 1998. Time-dependent models of U-Th-He and K-Ar evolution and the layering of mantle convection. Chem. Geol. 145, 413–429.
Albers, M., Christensen, U.R., 1996. The excess temperature of plumes rising from the core-mantle boundary. Geophys. Res. Lett. 23, 3567–3570.
Allegre, C.J., 1982. Chemical geodynamics. Tectonophysics 81, 109–132.
Allegre, C.J., Turcotte, D.L., 1986. Implications of a 2-component marble-cake mantle. Nature 323, 123–127.
Ammann, M.W., Brodholt, J.P., Wookey, J., Dobson, D.P., 2010. First-principles constraints on diffusion in lower-mantle minerals and a weak D″ layer. Nature 465, 462–465.
Andrault, D., Pesce, G., Bouhifd, M.A., Bolfan-Casanova, N., Henot, J.M., Mezouar, M., 2014. Melting of subducted basalt at the core-mantle boundary. Science 344, 892–895.
Antolik, M., Gu, Y.J., Ekstrom, G., Dziewonski, A.M., 2003. J362D28: a new joint model of compressional and shear velocity in the Earth's mantle. Geophys. J. Int. 153, 443–466.
Austermann, J., Kaye, B.T., Mitrovica, J.X., Huybers, P., 2014. A statistical analysis of the correlation between large igneous provinces and lower mantle seismic structure. Geophys. J. Int. 197, 1–9.
Ballmer, M.D., Schmerr, N.C., Nakagawa, T., Ritsema, J., 2015. Compositional mantle layering revealed by slab stagnation at ~1000-km depth. Sci. Adv. 1, e1500815.
Ballmer, M.D., Houser, C., Hernlund, J.W., Wentzcovitch, R.M., Hirose, K., 2017. Persistence of strong silica-enriched domains in the Earth's lower mantle. Nat. Geosci. 10, 236–241.
Le Bars, M., Davaille, A., 2004. Whole layer convection in a heterogeneous planetary mantle. J. Geophys. Res. B 109. http://dx.doi.org/10.1029/2003jb002617.
Becker, T.W., Boschi, L., 2002. A comparison of tomographic and geodynamic mantle models. Geochem. Geophys. Geosyst. 3. http://dx.doi.org/10.1029/2001gc000168.
Bercovici, D., Kelly, A., 1997. The non-linear initiation of diapirs and plume heads. Phys. Earth Planet. Inter. 101, 119–130.
Bijwaard, H., Spakman, W., 1999. Tomographic evidence for a narrow whole mantle plume below Iceland. Earth Planet. Sci. Lett. 166, 121–126.
Boschi, L., Becker, T.W., Steinberger, B., 2007. Mantle plumes: dynamic models and seismic images. Geochem. Geophys. Geosyst. 8. http://dx.doi.org/10.1029/2007gc001733.
Bower, D.J., Wicks, J.K., Gurnis, M., Jackson, J.M., 2011. A geodynamic and mineral physics model of a solid-state ultralow-velocity zone. Earth Planet. Sci. Lett. 303, 193–202.
Bower, D.J., Gurnis, M., Seton, M., 2013. Lower mantle structure from paleogeographically constrained dynamic earth models. Geochem. Geophys. Geosyst. 14, 44–63.
Brandenburg, J.P., van Keken, P.E., 2007a. Deep storage of oceanic crust in a vigorously convecting mantle. J. Geophys. Res. B 112. http://dx.doi.org/10.1029/2006jb004813.
Brandenburg, J.P., van Keken, P.E., 2007b. Methods for thermochemical convection in Earth's mantle with force-balanced plates. Geochem. Geophys. Geosyst. 8. http://dx.doi.org/10.1029/2007gc001692.
Brandenburg, J.P., Hauri, E.H., van Keken, P.E., Ballentine, C.J., 2008. A multiple-system study of the geochemical evolution of the mantle with force-balanced plates and thermochemical effects. Earth Planet. Sci. Lett. 276, 1–13.
Breger, L., Romanowicz, B., 1998. Three-dimensional structure at the base of the mantle beneath the Central Pacific. Science 282, 718–720.
Buffett, B.A., Garnero, E.J., Jeanloz, R., 2000. Sediments at the top of Earth's core. Science 290, 1338–1342.
Bull, A.L., McNamara, A.K., Ritsema, J., 2009. Synthetic tomography of plume clusters and thermochemical piles. Earth Planet. Sci. Lett. 278, 152–162.
Bull, A.L., McNamara, A.K., Becker, T.W., Ritsema, J., 2010. Global scale models of the mantle flow field predicted by synthetic tomography models. Phys. Earth Planet. Inter. 182, 129–138.
Bunge, H.P., Richards, M.A., Lithgow-Bertelloni, C., Baumgardner, J.R., Grand, S.P., Romanowicz, B.A., 1998. Time scales and heterogeneous structure in geodynamic earth models. Science 280, 91–95.
Burke, K., Torsvik, T.H., 2004. Derivation of Large Igneous Provinces of the past 200 million years from long-term heterogeneities in the deep mantle. Earth Planet. Sci. Lett. 227, 531–538.
Burke, K., Steinberger, B., Torsvik, T.H., Smethurst, M.A., 2008. Plume generation zones at the margins of large low shear velocity provinces on the core-mantle boundary. Earth Planet. Sci. Lett. 265, 49–60.
Cabral, R.A., Jackson, M.G., Rose-Koga, E.F., Koga, K.T., Whitehouse, M.J., Antonelli, M.A., Farquhar, J., Day, J.M., Hauri, E.H., 2013. Anomalous Sulphur isotopes in plume lavas reveal deep mantle storage of Archaean crust. Nature 496, 490–493.
Campbell, I.H., Griffiths, R.W., 1990. Implications of mantle plume structure for the evolution of flood basalts. Earth Planet. Sci. Lett. 99, 79–93.
Campbell, I.H., Griffiths, R.W., Hill, R.I., 1989. Melting in an Archean mantle plume - heads its basalts, tails its komatiites. Nature 339, 697–699.
Carlson, R.W., 1994. Mechanisms of earth differentiation - consequences for the chemical-structure of the mantle. Rev. Geophys. 32, 337–361.
Christensen, U.R., Hofmann, A.W., 1994. Segregation of subducted oceanic-crust in the convecting mantle. J. Geophys. Res. B 99, 19867–19884.
Conrad, C.P., Steinberger, B., Torsvik, T.H., 2013. Stability of active mantle upwelling revealed by net characteristics of plate tectonics. Nature 498, 479–482.
Cottaar, S., Romanowicz, B., 2012. An unsually large ULVZ at the base of the mantle near Hawaii. Earth Planet. Sci. Lett. 355-356, 213–222.

Courtillot, V., Davaille, A., Besse, J., Stock, J., 2003. Three distinct types of hotspots in the Earth's mantle. Earth Planet. Sci. Lett. 205, 295–308.
Crameri, F., Tackley, P.J., 2014. Spontaneous development of arcuate single-sided subduction in global 3-D mantle convection models with a free surface. J. Geophys. Res. B 119, 5921–5942.
Crameri, F., Tackley, P.J., 2015. Parameters controlling dynamically self-consistent plate tectonics and single-sided subduction in global models of mantle convection. J. Geophys. Res. B 120, 3680–3706.
Crameri, F., Tackley, P.J., Meilick, I., Gerya, T.V., Kaus, B.J.P., 2012. A free plate surface and weak oceanic crust produce single-sided subduction on earth. Geophys. Res. Lett. 39. http://dx.doi.org/10.1029/2011gl050046.
Cserepes, L., Christensen, U.R., Ribe, N.M., 2000. Geoid height versus topography for a plume model of the Hawaiian swell. Earth Planet. Sci. Lett. 178, 29–38.
Davaille, A., 1999. Simultaneous generation of hotspots and superswells by convection in a heterogenous planetary mantle. Nature 402, 756–760.
Davaille, A., Girard, F., Le Bars, M., 2002. How to anchor hotspots in a convecting mantle? Earth Planet. Sci. Lett. 203, 621–634.
Davaille, A., Le Bars, M., Carbonne, C., 2003. Thermal convection in a heterogeneous mantle. Compt. Rendus Geosci. 335, 141–156.
Davaille, A., Stutzmann, E., Silveira, G., Besse, J., Courtillot, V., 2005. Convective patterns under the Indo-Atlantic < < box > > Earth Planet. Sci. Lett. 239, 233–252.
Davies, G.F., 1990. Mantle plumes, mantle stirring and hotspot chemistry. Earth Planet. Sci. Lett. 99, 94–109.
Davies, G.F., 1995. Penetration of plates and plumes through the mantle transition zone. Earth Planet. Sci. Lett. 133, 507–516.
Davies, G.F., 2008. Episodic layering of the early mantle by the 'basalt barrier' mechanism. Earth Planet. Sci. Lett. 275, 382–392.
Davies, D., Davies, J., 2009. Thermally-driven mantle plumes reconcile multiple hot-spot observations. Earth Planet. Sci. Lett. 278, 50–54.
Davies, G.F., Gurnis, M., 1986. Interaction of mantle dregs with convection - lateral heterogeneity at the core mantle boundary. Geophys. Res. Lett. 13, 1517–1520.
Davies, D.R., Goes, S., Davies, J.H., Schuberth, B.S.A., Bunge, H.P., Ritsema, J., 2012. Reconciling dynamic and seismic models of Earth's lower mantle: the dominant role of thermal heterogeneity. Earth Planet. Sci. Lett. 353-354, 253–269.
Demets, C., Gordon, R.G., Argus, D.F., Stein, S., 1994. Effect of recent revisions to the geomagnetic reversal time-scale on estimates of current plate motions. Geophys. Res. Lett. 21, 2191–2194.
van der Hilst, R.D., Karason, H., 1999. Compositional heterogeneity in the bottom 1000 kilometers of Earth's mantle: toward a hybrid convection model. Science 283, 1885–1888.
Deschamps, F., Tackley, P.J., 2008. Searching for models of thermo-chemical convection that explain probabilistic tomography I. Principles and influence of rheological parameters. Phys. Earth Planet. Inter. 171, 357–373.
Deschamps, F., Tackley, P.J., 2009. Searching for models of thermo-chemical convection that explain probabilistic tomography. II-Influence of physical and compositional parameters. Phys. Earth Planet. Inter. 176, 1–18.
Deschamps, F., Trampert, J., 2003. Mantle tomography and its relation to temperature and composition. Phys. Earth Planet. Inter. 140, 277–291.
Deschamps, F., Kaminski, E., Tackley, P.J., 2011. A deep mantle origin for the primitive signature of ocean island basalt. Nat. Geosci. 4, 879–882.
Dobson, D.P., Brodholt, J.P., 2005. Subducted banded iron formations as a source of ultralow-velocity zones at the core-mantle boundary. Nature 434, 371–374.
Doubrovine, P.V., Steinberger, B., Torsvik, T.H., 2016. A failure to reject: testing the correlation between large igneous provinces and deep mantle structures with EDF statistics. Geochem. Geophys. Geosyst. 17, 1130–1163.
Duncan, R.A., Richards, M.A., 1991. Hotspots, mantle plumes, flood basalts, and true polar wander. Rev. Geophys. 29, 31–50.
Dziewonski, A.M., Hager, B.H., Oconnell, R.J., 1977. Large-scale heterogeneities in lower mantle. J. Geophys. Res. B 82, 239–255.
Dziewonski, A.M., Lekic, V., Romanowicz, B.A., 2010. Mantle Anchor Structure: an argument for bottom up tectonics. Earth Planet. Sci. Lett. 299, 69–79.
Farnetani, C.G., Hofmann, A.W., 2009. Dynamics and internal structure of a lower mantle plume conduit. Earth Planet. Sci. Lett. 282, 314–322.
Farnetani, C.G., Richards, M.A., 1994. Numerical investigations of the mantle plume initiation model for flood-basalt events. J. Geophys. Res. B 99, 13813–13833.
Farnetani, D.G., Richards, M.A., 1995. Thermal entrainment and melting in mantle plumes. Earth Planet. Sci. Lett. 136, 251–267.
Farnetani, C.G., Samuel, H., 2003. Lagrangian structures and stirring in the Earth's mantle. Earth Planet. Sci. Lett. 206, 335–348.
Farnetani, C.G., Samuel, H., 2005. Beyond the thermal plume paradigm. Geophys. Res. Lett. 32. http://dx.doi.org/10.1029/2005gl022360.
Farnetani, C.G., Legras, B., Tackley, P.J., 2002. Mixing and deformations in mantle plumes. Earth Planet. Sci. Lett. 196, 1–15.
Farnetani, C.G., Hofmann, A.W., Class, C., 2012. How double volcanic chains sample geochemical anomalies from the lowermost mantle. Earth Planet. Sci. Lett. 359–360, 240–247.
Flament, N., Williams, S., Muller, R.D., Gurnis, M., Bower, D.J., 2017. Origin and evolution of the deep thermochemical structure beneath Eurasia. Nat. Commun. 8. http://dx.doi.org/10.1038/ncomms14164.
Ford, S.R., Garnero, E.J., McNamara, A.K., 2006. A strong lateral shear velocity gradient and anisotropy heterogeneity in the lowermost mantle beneath the southern Pacific. J. Geophys. Res. B 111. http://dx.doi.org/10.1029/2004jb003574.
French, S.W., Romanowicz, B., 2015. Broad plumes rooted at the base of the Earth's mantle beneath major hotspots. Nature 525, 95–99.
Garnero, E.J., Helmberger, D.V., 1996. Seismic detection of a thin laterally varying boundary layer at the base of the mantle beneath the central-Pacific. Geophys. Res. Lett. 23, 977–980.
Garnero, E.J., McNamara, A.K., 2008. Structure and dynamics of Earth's lower mantle. Science 320, 626–628.
Garnero, E.J., Vidale, J.E., 1999. ScP; a probe of ultralow velocity zones at the base of the mantle. Geophys. Res. Lett. 26, 377–380.
Garnero, E.J., Revenaugh, J., Williams, Q., Lay, T., Kellogg, L.H., 1998. Ultralow velocity zone at the core-mantle boundary. Geodynamics 28, 319–334.
Garnero, E.J., Kennett, B., Loper, D.E., 2005. Studies of the earth's deep interior—eighth symposium. Phys. Earth Planet. Inter. 153, 1–2.
Garnero, E.J., Thorne, M.S., McNamara, A.K., Rost, S., 2007. Fine-scale ultra-low velocity zone layering at the core-mantle boundary and superplumes. In: Yuen, D.A., Maruyama, S., Karato, S.-I., W., B.F. (Eds.), Superplumes: Beyond Plate Tectonics. Springer (p. 569).
Garnero, E.J., McNamara, A.K., Shim, S.H., 2016. Continent-sized anomalous zones with low seismic velocity at the base of Earth's mantle. Nat. Geosci. 9, 481–489.
Gonnermann, H.M., Mukhopadhyay, S., 2007. Non-equilibrium degassing and a primordial source for helium in ocean-island volcanism. Nature 449, 1037–1040.
Gonnermann, H.M., Mukhopadhyay, S., 2009. Preserving noble gases in a convecting mantle. Nature 459, 560–563.
Gonnermann, H.M., Jellinek, A.M., Richards, M.A., Manga, M., 2004. Modulation of mantle plumes and heat flow at the core mantle boundary by plate-scale flow: results from laboratory experiments. Earth Planet. Sci. Lett. 226, 53–67.
Graham, D.W., 2002. Noble gas isotope geochemistry of mid-ocean ridge and ocean island basalts: characterization of mantle source reservoirs. Rev. Mineral. Geochem. 47, 247–317.
Grand, S.P., 2002. Mantle shear-wave tomography and the fate of subducted slabs. Phil. Trans. R. Soc. A 360, 2475–2491.
Griffiths, R.W., Campbell, I.H., 1990. Stirring and structure in mantle starting plumes. Earth Planet. Sci. Lett. 99, 66–78.
Gurnis, M., 1986. The effects of chemical density differences on convective mixing in the earth's mantle. J. Geophys. Res. Solid Earth 91, 1407–1419.
Hart, S.R., 1971. The geochemistry of basaltic rocks. Year B. Carnegie Inst. Wash. 70, 353–355.
He, Y.M., Wen, L.X., 2009. Structural features and shear-velocity structure of the "Pacific Anomaly". J. Geophys. Res. B 114. http://dx.doi.org/10.1029/2008jb005814.
He, Y.M., Wen, L.X., 2012. Geographic boundary of the "Pacific Anomaly" and its geometry and transitional structure in the north. J. Geophys. Res. B 117. http://dx.doi.org/10.1029/2012jb009436.
He, Y.M., Wen, L.X., Zheng, T.Y., 2006. Geographic boundary and shear wave velocity structure of the "Pacific anomaly" near the core-mantle boundary beneath western Pacific. Earth Planet. Sci. Lett. 244, 302–314.
Hernlund, J.W., Houser, C., 2008. The statistical distribution of seismic velocities in Earth's deep mantle. Earth Planet. Sci. Lett. 265, 423–437.
Hernlund, J.W., McNamara, A.K., 2015. The core–mantle boundary region. In: Schubert, G. (Ed.), Treatise on Geophysics, 2nd edition. Elsevier, Oxford, pp. 461–519.
Hernlund, J.W., Tackley, P.J., 2007. Some dynamical consequences of partial melting in Earth's deep mantle. Phys. Earth Planet. Inter. 162, 149–163.
Hirose, K., Fei, Y.W., Ma, Y.Z., Mao, H.K., 1999. The fate of subducted basaltic crust in the Earth's lower mantle. Nature 397, 53–56.
Hirose, K., Takafuji, N., Sata, N., Ohishi, Y., 2005. Phase transition and density of subducted MORB crust in the lower mantle. Earth Planet. Sci. Lett. 237, 239–251.
Hofmann, A.W., 1997. Mantle geochemistry: the message from oceanic volcanism. Nature 385, 219–229.
Hofmann, A.W., White, W.M., 1982. Mantle plumes from ancient oceanic-crust. Earth Planet. Sci. Lett. 57, 421–436.
Houser, C., Masters, G., Shearer, P., Laske, G., 2008. Shear and compressional velocity models of the mantle from cluster analysis of long-period waveforms. Geophys. J. Int. 174, 195–212.
Hu, Q., Kim, D.Y., Yang, W., Yang, L., Meng, Y., Zhang, L., Mao, H.K., 2016. FeO2 and FeOOH under deep lower-mantle conditions and Earth's oxygen-hydrogen cycles. Nature 534, 241–244.
Huang, J., Davies, G.F., 2007. Stirring in three-dimensional mantle convection models and implications for geochemistry: 2. Heavy tracers. Geochem. Geophys. Geosyst. 8. http://dx.doi.org/10.1029/2007GC001621.
Hunt, S.A., Davies, D.R., Walker, A.M., McCormack, R.J., Wills, A.S., Dobson, D.P., Li, L., 2012. On the increase in thermal diffusivity caused by the perovskite to post-perovskite phase transition and its implications for mantle dynamics. Earth Planet. Sci. Lett. 319–320, 96–103.
Ishii, M., Tromp, J., 1999. Normal-mode and free-air gravity constraints on lateral variations in velocity and density of Earth's mantle. Science 285, 1231–1236.
Ishii, M., Tromp, J., 2001. Even-degree lateral variations in the Earth's mantle constrained by free oscillations and the free-air gravity anomaly. Geophys. J. Int. 145, 77–96.
Ishii, M., Tromp, J., 2004. Constraining large-scale mantle heterogeneity using mantle and inner-core sensitive normal modes. Phys. Earth Planet. Inter. 146, 113–124.
Jackson, M.G., Hart, S.R., Konter, J.G., Kurz, M.D., Blusztajn, J., Farley, K.A., 2014. Helium and lead isotopes reveal the geochemical geometry of the Samoan plume. Nature 514, 355–358.
Jellinek, A.M., Manga, M., 2002. The influence of a chemical boundary layer on the fixity, spacing and lifetime of mantle plumes. Nature 418, 760–763.
Jellinek, A.M., Manga, M., 2004. Links between long-lived hot spots, mantle plumes, D″, and plate tectonics. Rev. Geophys. 42. http://dx.doi.org/10.1029/2003rg000144.
Jellinek, A.M., Gonnermann, H.M., Richards, M.A., 2003. Plume capture by divergent plate motions: implications for the distribution of hotspots, geochemistry of mid-ocean ridge basalts, and estimates of the heat flux at the core-mantle boundary. Earth Planet. Sci. Lett. 205, 361–378.
van Keken, P., 1997. Evolution of starting mantle plumes: a comparison between

numerical and laboratory models. Earth Planet. Sci. Lett. 148, 1–11.
van Keken, P.E., Gable, C.W., 1995. The interaction of a plume with a rheological boundary: a comparison between two- and three-dimensional models. J. Geophys. Res. B 100, 20291–20302.
Kellogg, L.H., Hager, B.H., van der Hilst, R.D., 1999. Compositional stratification in the deep mantle. Science 283, 1881–1884.
Kelly, A., Bercovici, D., 1997. The clustering of rising diapirs and plume heads. Geophys. Res. Lett. 24, 201–204.
Koelemeijer, P., Ritsema, J., Deuss, A., van Heijst, H.J., 2016. SP12RTS: a degree-12 model of shear- and compressional-wave velocity for Earth's mantle. Geophys. J. Int. 204, 1024–1039.
Koelemeijer, P., Deuss, A., Ritsema, J., 2017. Density structure of Earth's lowermost mantle from Stoneley mode splitting observations. Nat. Commun. 8. http://dx.doi.org/10.1038/ncomms15241.
Kumagai, I., Davaille, A., Kurita, K., 2007. On the fate of thermally buoyant mantle plumes at density interfaces. Earth Planet. Sci. Lett. 254, 180–193.
Kustowski, B., Ekstrom, G., Dziewonski, A.M., 2008. Anisotropic shear-wave velocity structure of the Earth's mantle: a global model. J. Geophys. Res. B 113. http://dx.doi.org/10.1029/2007jb005169.
Labrosse, S., Hernlund, J.W., Coltice, N., 2007. A crystallizing dense magma ocean at the base of the Earth's mantle. Nature 450, 866–869.
Lassak, T.M., McNamara, A.K., Zhong, S., 2007. Influence of thermochemical piles on topography at Earth's core-mantle boundary. Earth Planet. Sci. Lett. 261, 443–455.
Lassak, T.M., McNamara, A.K., Garnero, E.J., Zhong, S.J., 2010. Core-mantle boundary topography as a possible constraint on lower mantle chemistry and dynamics. Earth Planet. Sci. Lett. 289, 232–241.
Lau, H.C.P., Mitrovica, J.X., Davis, J.L., Tromp, J., Yang, H.Y., Al-Attar, D., 2017. Tidal tomography constrains Earth's deep-mantle buoyancy. Nature 551, 321–326.
Lay, T., Garnero, E.J., 2011. Deep mantle seismic modeling and imaging. Annu. Rev. Earth Planet. Sci. 39 (39), 91–123.
Lee, C.T.A., Luffi, P., Hoink, T., Li, J., Dasgupta, R., Hernlund, J., 2010. Upside-down differentiation and generation of a 'primordial' lower mantle. Nature 463, 930–933.
Lekic, V., Cottaar, S., Dziewonski, A., Romanowicz, B., 2012. Cluster analysis of global lower mantle tomography: a new class of structure and implications for chemical heterogeneity. Earth Planet. Sci. Lett. 357–358, 68–77.
Li, M., McNamara, A.K., 2013. The difficulty for subducted oceanic crust to accumulate at the Earth's core-mantle boundary. J. Geophys. Res. B 118, 1807–1816.
Li, X.D., Romanowicz, B., 1996. Global mantle shear velocity model developed using nonlinear asymptotic coupling theory. J. Geophys. Res. B 101, 22245–22272.
Li, C., van der Hilst, R.D., Engdahl, E.R., Burdick, S., 2008. A new global model for P wave speed variations in Earth's mantle. Geochem. Geophys. Geosyst. 9. http://dx.doi.org/10.1029/2007gc001806.
Li, M., McNamara, A.K., Garnero, E.J., 2014a. Chemical complexity of hotspots caused by cycling oceanic crust through mantle reservoirs. Nat. Geosci. 7, 366–370.
Li, Y., Deschamps, F., Tackley, P.J., 2014b. The stability and structure of primordial reservoirs in the lower mantle: insights from models of thermochemical convection in three-dimensional spherical geometry. Geophys. J. Int. 199, 914–930.
Li, Y., Deschamps, F., Tackley, P.J., 2015. Effects of the post-perovskite phase transition properties on the stability and structure of primordial reservoirs in the lower mantle of the earth. Earth Planet. Sci. Lett. 432, 1–12.
Li, Y., Deschamps, F., Tackley, J., 2016. Small post-perovskite patches at the base of lower mantle primordial reservoirs: insights from 2-D numerical modeling and implications for ULVZs. Geophys. Res. Lett. 43, 3215–3225.
Li, M., McNamara, A.K., Garnero, E.J., Yu, S., 2017. Compositionally-distinct ultra-low velocity zones on Earth's core-mantle boundary. Nat. Commun. 8. http://dx.doi.org/10.1038/s41467-41017-00219-x.
Lin, S.C., van Keken, P.E., 2005. Multiple volcanic episodes of flood basalts caused by thermochemical mantle plumes. Nature 436, 250–252.
Lin, S.C., van Keken, P.E., 2006. Dynamics of thermochemical plumes: 1. Plume formation and entrainment of a dense layer. Geochem. Geophys. Geosyst. 7. http://dx.doi.org/10.1029/2005gc001071.
Lithgow-Bertelloni, C., Richards, M.A., 1998. The dynamics of Cenozoic and Mesozoic plate motions. Rev. Geophys. 36, 27–78.
Liu, J., Li, J., Hrubiak, R., Smith, J.S., 2016. Origins of ultralow velocity zones through slab-derived metallic melt. Proc. Natl. Acad. Sci. U. S. A. 113, 5547–5551.
Lowman, J.P., King, S.D., Gable, C.W., 2004. Steady plumes in viscously stratified, vigorously convecting, three-dimensional numerical mantle convection models with mobile plates. Geochem. Geophys. Geosyst. 5. http://dx.doi.org/10.1029/2003gc000583.
Luo, S.N., Ni, S.D., Helmberger, D.V., 2001. Evidence for a sharp lateral variation of velocity at the core-mantle boundary from multipathed PKPab. Earth Planet. Sci. Lett. 189, 155–164.
Mao, W.L., Meng, Y., Shen, G.Y., Prakapenka, V.B., Campbell, A.J., Heinz, D.L., Shu, J.F., Caracas, R., Cohen, R.E., Fei, Y.W., Hemley, R.J., Mao, H.K., 2005. Iron-rich silicates in the Earth's D″ layer. Proc. Natl. Acad. Sci. U. S. A. 102, 9751–9753.
Mao, W.L., Mao, H.K., Sturhahn, W., Zhao, J.Y., Prakapenka, V.B., Meng, Y., Shu, J.F., Fei, Y.W., Hemley, R.J., 2006. Iron-rich post-perovskite and the origin of ultralow-velocity zones. Science 312, 564–565.
Masters, G., Laske, G., Bolton, H., Dziewonski, A., 2000. The relative behavior of shear velocity, bulk sound speed, and compressional velocity in the mantle: Implications for chemical and thermal structure. In: Karato, S., Forte, A., Lieberman, R., Masters, G., Stixrude, L. (Eds.), Earth's Deep Interior: Mineral Physics and Tomography from the Atomic to the Global Scale. American Geophysical Union (p. 289).
Matyska, C., Moser, J., Yuen, D.A., 1994. The potential influence of radiative heat-transfer on the formation of megaplumes in the lower mantle. Earth Planet. Sci. Lett. 125, 255–266.
McNamara, A.K., Zhong, S.J., 2004. Thermochemical structures within a spherical mantle: Superplumes or piles? J. Geophys. Res. B 109. http://dx.doi.org/10.1029/2003jb002847.
McNamara, A.K., Zhong, S.J., 2005. Thermochemical structures beneath Africa and the Pacific Ocean. Nature 437, 1136–1139.
McNamara, A.K., Garnero, E.J., Rost, S., 2010. Tracking deep mantle reservoirs with ultra-low velocity zones. Earth Planet. Sci. Lett. 299, 1–9.
Megnin, C., Romanowicz, B., 2000. The three-dimensional shear velocity structure of the mantle from the inversion of body, surface and higher-mode waveforms. Geophys. J. Int. 143, 709–728.
Mittelstaedt, E., Tackley, P.J., 2006. Plume heat flow is much lower than CMB heat flow. Earth Planet. Sci. Lett. 241, 202–210.
Montelli, R., Nolet, G., Dahlen, F.A., Masters, G., Engdahl, E.R., Hung, S.H., 2004. Finite-frequency tomography reveals a variety of plumes in the mantle. Science 303, 338–343.
Morgan, W.J., 1971. Convection plumes in lower mantle. Nature 230, 42–43.
Mosca, I., Cobden, L., Deuss, A., Ritsema, J., Trampert, J., 2012. Seismic and mineralogical structures of the lower mantle from probabilistic tomography. J. Geophys. Res. B 117. http://dx.doi.org/10.1029/2011jb008851.
Mukhopadhyay, S., 2012. Early differentiation and volatile accretion recorded in deep-mantle neon and xenon. Nature 486, 101–104.
Mulyukova, E., Steinberger, B., Dabrowski, M., Sobolev, S.V., 2015. Survival of LLSVPs for billions of years in a vigorously convecting mantle: replenishment and destruction of chemical anomaly. J. Geophys. Res. B 120, 3824–3847.
Nakagawa, T., Buffett, B.A., 2005. Mass transport mechanism between the upper and lower mantle in numerical simulations of thermochemical mantle convection with multicomponent phase changes. Earth Planet. Sci. Lett. 230, 11–27.
Nakagawa, T., Tackley, P.J., 2004. Thermo-chemical structure in the mantle arising from a three-component convective system and implications for geochemistry. Phys. Earth Planet. Inter. 146, 125–138.
Nakagawa, T., Tackley, P.J., 2005. The interaction between the post-perovskite phase change and a thermo-chemical boundary layer near the core-mantle boundary. Earth Planet. Sci. Lett. 238, 204–216.
Nakagawa, T., Tackley, P.J., 2006. Three-dimensional structures and dynamics in the deep mantle: effects of post-perovskite phase change and deep mantle layering. Geophys. Res. Lett. 33. http://dx.doi.org/10.1029/2006gl025719.
Nakagawa, T., Tackley, P.J., 2011. Effects of low-viscosity post-perovskite on thermo-chemical mantle convection in a 3-D spherical shell. Geophys. Res. Lett. 38. http://dx.doi.org/10.1029/2010gl046494.
Nakagawa, T., Tackley, P.J., Deschamps, F., Connolly, J.A.D., 2010. The influence of MORB and harzburgite composition on thermo-chemical mantle convection in a 3-D spherical shell with self-consistently calculated mineral physics. Earth Planet. Sci. Lett. 296, 403–412.
Ni, S.D., Helmberger, D.V., 2003a. Further constraints on the African superplume structure. Phys. Earth Planet. Inter. 140, 243–251.
Ni, S.D., Helmberger, D.V., 2003b. Ridge-like lower mantle structure beneath South Africa. J. Geophys. Res. B 108. http://dx.doi.org/10.1029/2001jb001545.
Ni, S.D., Helmberger, D.V., 2003c. Seismological constraints on the south African superplume; could be the oldest distinct structure on Earth. Earth Planet. Sci. Lett. 206, 119–131.
Ni, S.D., Tan, E., Gurnis, M., Helmberger, D., 2002. Sharp sides to the African superplume. Science 296, 1850–1852.
Ni, S.D., Helmberger, D.V., Tromp, J., 2005. Three-dimensional structure of the African superplume from waveform modelling. Geophys. J. Int. 161, 283–294.
Nomura, R., Ozawa, H., Tateno, S., Hirose, K., Hernlund, J., Muto, S., Ishii, H., Hiraoka, N., 2011. Spin crossover and iron-rich silicate melt in the Earth's deep mantle. Nature 473, 199–202.
Ohtani, E., Maeda, M., 2001. Density of basaltic melt at high pressure and stability of the melt at the base of the lower mantle. Earth Planet. Sci. Lett. 193, 69–75.
Olson, P., Schubert, G., Anderson, C., 1993. Structure of axisymmetric mantle plumes. J. Geophys. Res. 98, 6829–6844.
Porcelli, D., Ballentine, C.J., 2002. Models for the distribution of terrestrial noble gases and evolution of the atmosphere. Rev. Mineral. Geochem. 47, 411–480.
Pradhan, G.K., Fiquet, G., Siebert, J., Auzende, A.-L., Morard, G., Antonangeli, D., Garbarino, G., 2015. Melting of MORB at core–mantle boundary. Earth Planet. Sci. Lett. 431, 247–255.
Resovsky, J.S., Ritzwoller, M.H., 1999. Regularization uncertainty in density models estimated from normal mode data. Geophys. Res. Lett. 26, 2319–2322.
Ribe, N.M., Christensen, U.R., 1994. 3-dimensional modeling of plume-lithosphere interaction. J. Geophys. Res. B 99, 669–682.
Richards, M.A., Duncan, R.A., Courtillot, V.E., 1989. Flood basalts and hot-spot tracks - plume heads and tails. Science 246, 103–107.
Richards, M.A., Jones, D.L., Duncan, R.A., Depaolo, D.J., 1991. A mantle plume initiation model for the Wrangellia flood-basalt and other oceanic plateaus. Science 254, 263–267.
Ringwood, A.E., Irifune, T., 1988. Nature of the 650-km seismic discontinuity - implications for mantle dynamics and differentiation. Nature 331, 131–136.
Ritsema, J., Allen, R.M., 2003. The elusive mantle plume. Earth Planet. Sci. Lett. 207, 1–12.
Ritsema, J., van Heijst, H.J., 2002. Constraints on the correlation of P- and S-wave velocity heterogeneity in the mantle from P, PP, PPP and PKPab traveltimes. Geophys. J. Int. 149, 482–489.
Ritsema, J., Garnero, E., Lay, T., 1997. A strongly negative shear velocity gradient and lateral variability in the lowermost mantle beneath the Pacific. J. Geophys. Res. B 102, 20395–20411.
Ritsema, J., van Heijst, H.J., Woodhouse, J.H., 1999. Complex shear wave velocity

structure imaged beneath Africa and Iceland. Science 286, 1925–1928.
Ritsema, J., van Heijst, H.J., Woodhouse, J.H., 2004. Global transition zone tomography. J. Geophys. Res. B 109. http://dx.doi.org/10.1029/2003jb002610.
Ritsema, J., McNamara, A.K., Bull, A.L., 2007. Tomographic filtering of geodynamic models: implications for model interpretation and large-scale mantle structure. J. Geophys. Res. B 112. http://dx.doi.org/10.1029/2006jb004566.
Ritsema, J., Deuss, A., van Heijst, H.J., Woodhouse, J.H., 2011. S40RTS: a degree-40 shear-velocity model for the mantle from new Rayleigh wave dispersion, teleseismic traveltime and normal-mode splitting function measurements. Geophys. J. Int. 184, 1223–1236.
Rost, S., Garnero, E.J., Williams, Q., Manga, M., 2005. Seismological constraints on a possible plume root at the core-mantle boundary. Nature 435, 666–669.
Rost, S., Garnero, E.J., Williams, Q., 2006. Fine-scale ultralow-velocity zone structure from high-frequency seismic array data. J. Geophys. Res. B 111.
Samuel, H., Farnetani, C.G., 2003. Thermochemical convection and helium concentrations in mantle plumes. Earth Planet. Sci. Lett. 207, 39–56.
Schmerr, N., Garnero, E., 2006. Investigation of upper mantle discontinuity structure beneath the Central Pacific using SS precursors. J. Geophys. Res. B 111. http://dx.doi.org/10.1029/2005jb004197.
Schmerr, N., Garnero, E., McNamara, A., 2010. Deep mantle plumes and convective upwelling beneath the Pacific Ocean. Earth Planet. Sci. Lett. 294, 143–151.
Schubert, G., Anderson, C., Goldman, P., 1995. Mantle plume interaction with an endothermic phase-change. J. Geophys. Res. B 100, 8245–8256.
Schubert, G., Masters, G., Olson, P., Tackley, P., 2004. Superplumes or plume clusters? Phys. Earth Planet. Inter. 146, 147–162.
Schuberth, B.S.A., Bunge, H.P., Ritsema, J., 2009. Tomographic filtering of high-resolution mantle circulation models: can seismic heterogeneity be explained by temperature alone? Geochem. Geophys. Geosyst. 10. http://dx.doi.org/10.1029/2009gc002401.
Scotese, C.R., Gahagan, L.M., Larson, R.L., 1988. Plate tectonic reconstructions of the cretaceous and Cenozoic ocean basins. Tectonophysics 155, 27–48.
Seton, M., Müller, R.D., Zahirovic, S., Gaina, C., Torsvik, T., Shephard, G., Talsma, A., Gurnis, M., Turner, M., Maus, S., Chandler, M., 2012. Global continental and ocean basin reconstructions since 200Ma. Earth Sci. Rev. 113, 212–270.
Shen, Y., Solomon, S.C., Bjarnason, I.T., Wolfe, C.J., 1998. Seismic evidence for a lower-mantle origin of the Iceland plume. Nature 395, 62–65.
Shen, Y., Wolfe, C.J., Solomon, S.C., 2003. Seismological evidence for a mid-mantle discontinuity beneath Hawaii and Iceland. Earth Planet. Sci. Lett. 214, 143–151.
Simmons, N.A., Forte, A.M., Boschi, L., Grand, S.P., 2010. GyPSuM: a joint tomographic model of mantle density and seismic wave speeds. J. Geophys. Res. B 115. http://dx.doi.org/10.1029/2010jb007631.
Sleep, N.H., 1990. Hotspots and mantle plumes: some phenomenology. J. Geophys. Res. 95, 6715–6736.
Sleep, N.H., 2006. Mantle plumes from top to bottom. Earth Sci. Rev. 77, 231–271.
Sleep, N.H., Richards, M.A., Hager, B.H., 1988. Onset of mantle plumes in the presence of preexisting convection. J. Geophys. Res. Solid Earth 93, 7672–7689.
Steinberger, B., 2000. Plumes in a convecting mantle: models and observations for individual hotspots. J. Geophys. Res. B 105, 11127–11152.
Steinberger, B., Torsvik, T.H., 2008. Absolute plate motions and true polar wander in the absence of hotspot tracks. Nature 452, 620–623.
Steinberger, B., Torsvik, T.H., 2012. A geodynamic model of plumes from the margins of large low shear velocity provinces. Geochem. Geophys. Geosyst. 13. http://dx.doi.org/10.1029/2011gc003808.
Steinberger, B., Sutherland, R., O'Connell, R.J., 2004. Prediction of Emperor-Hawaii seamount locations from a revised model of global plate motion and mantle flow. Nature 430, 167–173.
Stixrude, L., Lithgow-Bertelloni, C., 2005. Thermodynamics of mantle minerals - I. Physical properties. Geophys. J. Int. 162, 610–632.
Su, W.J., Dziewonski, A.M., 1997. Simultaneous inversion for 3-D variations in shear and bulk velocity in the mantle. Phys. Earth Planet. Inter. 100, 135–156.
Sun, D., Tan, E., Helmberger, D., Gurnis, M., 2007a. Seismological support for the metastable superplume model, sharp features, and phase changes within the lower mantle. Proc. Natl. Acad. Sci. U. S. A. 104, 9151–9155.
Sun, X.L., Song, D.X., Zheng, S.H., Helmberger, D.V., 2007b. Evidence for a chemical-thermal structure at base of mantle from sharp lateral P-wave variations beneath Central America. Proc. Natl. Acad. Sci. U. S. A. 104, 26–30.
Sun, D.Y., Helmberger, D., Ni, S.D., Bower, D., 2009. Direct measures of lateral velocity variation in the deep earth. J. Geophys. Res. B 114. http://dx.doi.org/10.1029/2008jb005873.
Tackley, P.J., 1998. Three-dimensional simulations of mantle convection with a thermo-chemical basal boundary layer: D″? In: Gurnis, M., Wysession, M.E., Knittle, E., Buffett, B.A. (Eds.), The Core-Mantle Boundary Region. American Geophysical Union (p. 334).
Tackley, P.J., 2000. Mantle convection and plate tectonics: toward an integrated physical and chemical theory. Science 288, 2002–2007.
Tackley, P.J., 2002. Strong heterogeneity caused by deep mantle layering. Geochem. Geophys. Geosyst. 3. http://dx.doi.org/10.1029/2001gc000167.
Tackley, P.J., 2007. Mantle geochemical geodynamics. In: Bercovici, D., Schubert, G. (Eds.), Treatise on Geophysics Volume 7: Mantle Dynamics. Elsevier, pp. 437–505.
Tackley, P.J., 2011. Living dead slabs in 3-D: the dynamics of compositionally-stratified slabs entering a "slab graveyard" above the core-mantle boundary. Phys. Earth Planet. Inter. 188, 150–162.
Tackley, P.J., 2012. Dynamics and evolution of the deep mantle resulting from thermal, chemical, phase and melting effects. Earth Sci. Rev. 110, 1–25.
Takeuchi, N., 2007. Whole mantle SH velocity model constrained by waveform inversion based on three-dimensional born kernels. Geophys. J. Int. 169, 1153–1163.
Tan, E., Gurnis, M., 2005. Metastable superplumes and mantle compressibility. Geophys. Res. Lett. 32. http://dx.doi.org/10.1029/2005gl024190.
Tan, E., Gurnis, M., 2007. Compressible thermochemical convection and application to lower mantle structures. J. Geophys. Res. B 112. http://dx.doi.org/10.1029/2006jb004505.
Tan, E., Gurnis, M., Han, L.J., 2002. Slabs in the lower mantle and their modulation of plume formation. Geochem. Geophys. Geosyst. 3. http://dx.doi.org/10.1029/2001gc000238.
Tan, E., Leng, W., Zhong, S.J., Gurnis, M., 2011. On the location of plumes and lateral movement of thermochemical structures with high bulk modulus in the 3-D compressible mantle. Geochem. Geophys. Geosyst. 12. http://dx.doi.org/10.1029/2011gc003665.
Thompson, P.F., Tackley, P.J., 1998. Generation of mega-plumes from the core-mantle boundary in a compressible mantle with temperature-dependent viscosity. Geophys. Res. Lett. 25, 1999–2002.
Thorne, M.S., Garnero, E.J., 2004. Inferences on ultralow-velocity zone structure from a global analysis ofSPdKSwaves. J. Geophys. Res. B 109. http://dx.doi.org/10.1029/2004jb003010.
Thorne, M.S., Garnero, E.J., Grand, S.P., 2004. Geographic correlation between hot spots and deep mantle lateral shear-wave velocity gradients. Phys. Earth Planet. Inter. 146, 47–63.
Thorne, M.S., Garnero, E.J., Jahnke, G., Igel, H., McNamara, A.K., 2013. Mega ultra low velocity zone and mantle flow. Earth Planet. Sci. Lett. 364, 59–67.
To, A., Romanowicz, B., Capdeville, Y., Takeuchi, N., 2005. 3D effects of sharp boundaries at the borders of the African and Pacific Superplumes: observation and modeling. Earth Planet. Sci. Lett. 233, 137–153.
Tolstikhin, I., Hofmann, A.W., 2005. Early crust on top of the Earth's core. Phys. Earth Planet. Inter. 148, 109–130.
Tolstikhin, I.N., Kramers, J.D., Hofmann, A.W., 2006. A chemical earth model with whole mantle convection: the importance of a core-mantle boundary layer (D″) and its early formation. Chem. Geol. 226, 79–99.
Torsvik, T.H., Müller, R.D., Van der Voo, R., Steinberger, B., Gaina, C., 2008a. Global plate motion frames: toward a unified model. Rev. Geophys. 46. http://dx.doi.org/10.1029/2007rg000227.
Torsvik, T.H., Smethurst, M.A., Burke, K., Steinberger, B., 2008b. Long term stability in deep mantle structure: evidence from the similar to 300 Ma Skagerrak-Centered Large Igneous Province (the SCLIP). Earth Planet. Sci. Lett. 267, 444–452.
Torsvik, T.H., Burke, K., Steinberger, B., Webb, S.J., Ashwal, L.D., 2010a. Diamonds sampled by plumes from the core-mantle boundary. Nature 466, 352–355.
Torsvik, T.H., Steinberger, B., Gurnis, M., Gaina, C., 2010b. Plate tectonics and net lithosphere rotation over the past 150My. Earth Planet. Sci. Lett. 291, 106–112.
Torsvik, T.H., van der Voo, R., Doubrovine, P.V., Burke, K., Steinberger, B., Ashwal, L.D., Tronnes, R.G., Webb, S.J., Bull, A.L., 2014. Deep mantle structure as a reference frame for movements in and on the Earth. Proc. Natl. Acad. Sci. U. S. A. 111, 8735–8740.
Trampert, J., Vacher, P., Vlaar, N., 2001. Sensitivities of seismic velocities to temperature, pressure and composition in the lower mantle. Phys. Earth Planet. Inter. 124, 255–267.
Trampert, J., Deschamps, F., Resovsky, J., Yuen, D., 2004. Probabilistic tomography maps chemical heterogeneities throughout the lower mantle. Science 306, 853–856.
Wang, Y., Wen, L.X., 2004. Mapping the geometry and geographic distribution of a very low velocity province at the base of the Earth's mantle. J. Geophys. Res. B 109. http://dx.doi.org/10.1029/2003jb002674.
Wang, Y., Wen, L.X., 2007. Geometry and P and S velocity structure of the "African Anomaly". J. Geophys. Res. B 112. http://dx.doi.org/10.1029/2006jb004483.
Weis, D., Garcia, M.O., Rhodes, J.M., Jellinek, M., Scoates, J.S., 2011. Role of the deep mantle in generating the compositional asymmetry of the Hawaiian mantle plume. Nat. Geosci. 4, 831–838.
Wen, L.X., 2001. Seismic evidence for a rapidly varying compositional anomaly at the base of the Earth's mantle beneath the Indian Ocean. Earth Planet. Sci. Lett. 194, 83–95.
Wen, L.X., 2002. An SH hybrid method and shear velocity structures in the lowermost mantle beneath the central Pacific and South Atlantic Oceans. J. Geophys. Res. B 107.
Wen, L.X., Silver, P., James, D., Kuehnel, R., 2001. Seismic evidence for a thermo-chemical boundary at the base of the Earth's mantle. Earth Planet. Sci. Lett. 189, 141–153.
White, W.M., 1985. Sources of oceanic basalts - radiogenic isotopic evidence. Geology 13, 115–118.
White, W.M., 2015a. Isotopes, DUPAL, LLSVPs, and Anekantavada. Chem. Geol. 419, 10–28.
White, W.M., 2015b. Probing the earth's deep interior through geochemistry. Geochem. Perspect. 95–251.
Wicks, J.K., Jackson, J.M., Sturhahn, W., 2010. Very low sound velocities in iron-rich (Mg,Fe)O: Implications for the core-mantle boundary region. Geophys. Res. Lett. 37. http://dx.doi.org/10.1029/2010gl043689.
Wicks, J., Jackson, J.M., Sturhahn, W., Zhang, D., 2017. Sound velocity and density of magnesiowüstites: implications for ultralow-velocity zone topography. Geophys. Res. Lett. http://dx.doi.org/10.1002/2016gl071225.
Williams, Q., Garnero, E.J., 1996. Seismic evidence for partial melt at the base of Earth's mantle. Science 273, 1528–1530.
Williams, Q., Revenaugh, J., Garnero, E., 1998. A correlation between ultra-low basal velocities in the mantle and hot spots. Science 281, 546–549.
Williams, C.D., Li, M., McNamara, A.K., Garnero, E.J., van Soest, M.C., 2015. Episodic entrainment of deep primordial mantle material into ocean island basalts. Nat. Commun. 6. http://dx.doi.org/10.1038/ncomms9937.
Wolfe, C.J., Bjarnason, I.T., VanDecar, J.C., Solomon, S.C., 1997. Seismic structure of the

Iceland mantle plume. Nature 385, 245–247.
Wolfe, C.J., Solomon, S.C., Laske, G., Collins, J.A., Detrick, R.S., Orcutt, J.A., Bercovici, D., Hauri, E.H., 2009. Mantle shear-wave velocity structure beneath the Hawaiian hot spot. Science 326, 1388–1390.
Wolfe, C.J., Solomon, S.C., Laske, G., Collins, J.A., Detrick, R.S., Orcutt, J.A., Bercovici, D., Hauri, E.H., 2011. Mantle P-wave velocity structure beneath the Hawaiian hot-spot. Earth Planet. Sci. Lett. 303, 267–280.
Xie, S.X., Tackley, P.J., 2004a. Evolution of helium and argon isotopes in a convecting mantle. Phys. Earth Planet. Inter. 146, 417–439.
Xie, S.X., Tackley, P.J., 2004b. Evolution of U-Pb and Sm-Nd systems in numerical models of mantle convection and plate tectonics. J. Geophys. Res. B 109. http://dx.doi.org/10.1029/2004jb003176.
Yang, T., Shen, Y., Vanderlee, S., Solomon, S., Hung, S., 2006. Upper mantle structure beneath the Azores hotspot from finite-frequency seismic tomography. Earth Planet. Sci. Lett. 250, 11–26.
Yuan, K., Romanowicz, B., 2017. Seismic evidence for partial melting at the root of major hot spot plumes. Science 357, 393–397.
Zhang, N., Zhong, S.J., 2011. Heat fluxes at the Earth's surface and core-mantle boundary since Pangea formation and their implications for the geomagnetic superchrons. Earth Planet. Sci. Lett. 306, 205–216.
Zhang, N., Zhong, S.J., Leng, W., Li, Z.X., 2010. A model for the evolution of the Earth's mantle structure since the early Paleozoic. J. Geophys. Res. B 115. http://dx.doi.org/10.1029/2009jb006896.
Zhao, C., Garnero, E.J., McNamara, A.K., Schmerr, N., Carlson, R.W., 2015. Seismic evidence for a chemically distinct thermochemical reservoir in Earth's deep mantle beneath Hawaii. Earth Planet. Sci. Lett. 426, 143–153.
Zhong, S.J., 2006. Constraints on thermochemical convection of the mantle from plume heat flux, plume excess temperature, and upper mantle temperature. J. Geophys. Res. B 111. http://dx.doi.org/10.1029/2005jb003972.
Zhong, S.J., Hager, B.H., 2003. Entrainment of a dense layer by thermal plumes. Geophys. J. Int. 154, 666–676.
Zhong, S.J., Watts, A.B., 2002. Constraints on the dynamics of mantle plumes from uplift of the Hawaiian islands. Earth Planet. Sci. Lett. 203, 105–116.